



Contents lists available at SciVerse ScienceDirect

NeuroImage

journal homepage: [www.elsevier.com/locate/ynimg](http://www.elsevier.com/locate/ynimg)

Comments and Controversies

## White matter integrity, fiber count, and other fallacies: The do's and don'ts of diffusion MRI

Derek K. Jones<sup>a,b,\*</sup>, Thomas R. Knösche<sup>c</sup>, Robert Turner<sup>c</sup>

<sup>a</sup> Cardiff University Brain Research Imaging Centre (CUBRIC), School of Psychology, Cardiff University, Park Place, Cardiff, CF10 3AT, UK

<sup>b</sup> Neuroscience and Mental Health Research Institute, Cardiff University, Cardiff, CF10 3AT, UK

<sup>c</sup> Max Planck Institute for Human Cognitive and Brain Sciences, Stephanstrasse 1A, 04013 Leipzig, Germany

### ARTICLE INFO

#### Article history:

Accepted 26 June 2012

Available online xxx

### ABSTRACT

Diffusion-weighted MRI (DW-MRI) has been increasingly used in imaging neuroscience over the last decade. An early form of this technique, diffusion tensor imaging (DTI) was rapidly implemented by major MRI scanner companies as a scanner selling point. Due to the ease of use of such implementations, and the plausibility of some of their results, DTI was leapt on by imaging neuroscientists who saw it as a powerful and unique new tool for exploring the structural connectivity of human brain. However, DTI is a rather approximate technique, and its results have frequently been given implausible interpretations that have escaped proper critique and have appeared misleadingly in journals of high reputation. In order to encourage the use of improved DW-MRI methods, which have a better chance of characterizing the actual fiber structure of white matter, and to warn against the misuse and misinterpretation of DTI, we review the physics of DW-MRI, indicate currently preferred methodology, and explain the limits of interpretation of its results. We conclude with a list of 'Do's and Don'ts' which define good practice in this expanding area of imaging neuroscience.

© 2012 Elsevier Inc. All rights reserved.

### Introduction

Diffusion weighted MRI (DW-MRI) (Behrens and Johansen-Berg, 2009; Jones, 2010a; Le Bihan and Breton, 1985; Le Bihan et al., 1986) is currently the only method capable of mapping the fiber<sup>1</sup> architecture of tissue (e.g., nervous tissue, muscle) *in vivo* and, as such, it has triggered tremendous hopes and expectations. As the technique has matured, an increasing number of software packages have been developed that allow such data to be analyzed in a push-button manner – sometimes to such an extent that the end-user need not know anything about the underlying physics, and yet are still able to derive a p-value which can be interpreted according to the hypotheses being tested. There are, however, a substantial number of pitfalls associated with these methods (see, e.g., Jones, 2010b, 2010c; Jones and Cercignani, 2010; Le Bihan et al., 2006), which can lead to biased or, in some cases, completely fallacious conclusions being drawn. What is not in question, however, is that DW-MRI carries invaluable *in vivo* information about tissue microstructure, but in order to extract this information in the most efficient and unbiased way, it is important to make the right choices for the acquisition and analysis of these data, and, even more importantly, for the *interpretation* of the results.

It is in this context that this article focuses on three issues. The first of these is: What exactly are we measuring with DW-MRI, *i.e.*, what is

the immediate meaning of the data we get from the technique? The second is: What questions are we trying to answer on the basis of DW-MRI? The link between these two issues is the basis for the third issue, interpretation. Our main focus is on measurements within white matter of the live human brain, although many of the issues discussed here are equally relevant to pre-clinical studies in animal models, and of tissues other than brain.

The target audience of this article is the typical 'end user' who has access to diffusion-weighted MR sequences, provided by the MR scanner manufacturer, and uses 'push-button' software packages to analyze their data to look for group differences or structure–function correlations. It is our opinion that, without basic insight into the fundamental principles of the method and, most importantly, its limitations and pitfalls, misunderstandings, misconceptions and misinterpretation will be perpetuated. Our aim is to provide this grounding to the aforementioned target audience.

### What does diffusion-weighted MR imaging actually measure?

Diffusion-weighted MRI measures just one thing – the dephasing of spins of protons in the presence of a spatially-varying magnetic field ('gradient'). The mechanism of interest here is the phase change resulting from components of incoherent displacement of spins along the axis of the applied field gradient, which changes their Larmor frequency. The longer the protons are allowed to diffuse (the 'diffusion time',  $\Delta$ ) and the higher the mean squared displacement per unit time

\* Corresponding author. Fax: +44 (0) 29 2087 0339.

E-mail address: [jonesd27@Cardiff.ac.uk](mailto:jonesd27@Cardiff.ac.uk) (D.K. Jones).

<sup>1</sup> In nervous tissue, we use the term 'fiber' to refer to one or several axons.

of the molecules (the ‘apparent diffusivity’), the more the molecules will distribute over different distances from the origin with different associated phase shifts. This phase dispersion leads to a loss of signal coherence and therefore a reduction in signal amplitude. By comparing the signal amplitude with and without the diffusion-encoding gradient applied, the portion of dephasing resulting from incoherent motion during the application of the gradient can be isolated. The signal attenuation depends on: (i) the distribution of displacements during the diffusion time ( $\Delta$ ) along the axis of the applied gradient; and (ii) the gradient strength and duration, which determine the sensitivity of the signal phase towards displacement. Since diffusion time ( $\Delta$ ), gradient duration ( $\delta$ ), and gradient strength are all known (and usually combined to derive the ‘b-value’; Le Bihan and Breton, 1985) we have some kind of correlate for the motion of the diffusing particles along a particular axis.<sup>2</sup>

As shown by Cory and Garroway (1990) as well as Callaghan et al. (1991), under the so-called narrow pulse assumption (i.e.,  $\delta \ll \Delta$ ), the probability density that a particle has moved to a certain point within a given diffusion time (the diffusion propagator) can be described by the Fourier transform of the signal attenuation. As an important consequence, estimation of the diffusion propagator need not invoke any modeling assumptions. However, full reconstruction of the diffusion propagator is not possible, as it would require infinite sampling of the q-space (space spanned by gradient directions and b-values). Reasonable approximation of the diffusion propagator in three-dimensions is possible and requires diffusion-induced dephasing to be measured along multiple axes and at multiple strengths (b-values) of diffusion-weighting. Combined with imaging, this allows one to make spatial maps of quantities derived from the 3D-propagator (Callaghan et al., 1988; Wedeen et al., 2005). A more general and complete description of the diffusion-weighted signal, for arbitrary gradient wave-forms (i.e., whether or not the narrow-pulse approximation is valid), is to use the cumulant expansion (Stepisnik, 1981; van Kampen, 1974), in which the logarithm of the diffusion-weighted signal is expanded in powers of the diffusion-gradient in the vicinity of zero gradient amplitude (Kiselev, 2010; Liu et al., 2003).

In practice, however, due to the aforementioned time constraints on *in vivo* imaging of humans, it is not usually possible to acquire sufficient data to reconstruct a reasonable estimate of the full three-dimensional propagator, or to estimate all cumulants. Hence, the majority of DW-MRI studies tend to use a single diffusion weighting when measuring signal attenuation along different axes. Since each encoding vector has equal magnitude, the ‘tips’ of the encoding vector lie on the surface of a sphere – and so such approaches are referred to as ‘single shell’ acquisitions. As such, single-shell acquisitions yield much more limited information on the dispersion of the diffusion distances, within the experimental diffusion time, along the axis of the applied encoding gradient.

So, what is the signal attenuation sensitive to? First, it reflects the general mobility of water molecules, depending on temperature, viscosity, presence of large molecules, and many other factors. More interestingly, it also depends on barriers and obstacles imposed by microstructure, e.g., cell membranes, myelin sheaths and microtubules (Beaulieu, 2002). Such barriers slow down the diffusing particles (‘hindered diffusion’) or even impose an upper limit on their overall mean-square displacement (‘restricted diffusion’).<sup>3</sup> Exactly how this

<sup>2</sup> At this stage, we feel it is important to stress that if there is any component of displacement along the applied gradient axis, then this will lead to signal attenuation. In other words, if the gradient is applied along axis  $\mathbf{r}$ , water molecules do not have to be moving parallel to  $\mathbf{r}$  to cause signal loss. This is a point that appears to be often misunderstood in the literature. Only when the displacement is perfectly perpendicular to the encoding axis will there be no contribution to signal loss – since it is only at this orientation that there is no component of displacement along the encoding axis.

<sup>3</sup> This distinction between restriction and hindrance is important when interpreting diffusion MR signals. There is a tendency for the term ‘restricted’ to be used in the context of diffusion tensor imaging – but, while the tensor parameters are influenced by both restricted and hindered diffusion, the tensor model assumes Gaussianity and therefore translates restricted into hindered diffusion.

restriction and hindrance influence the signal is an open and complicated question and, as such, one is forced to invoke a number of modeling assumptions – which may or may not be correct. The only thing that we can say with absolute certainty is that DW-MRI measurements reflect the amount of hindrance/restriction experienced by water molecules moving with a component of displacement along the axis of the applied gradient, averaged over the voxel. Unfortunately, this is about it – anything more has to involve modeling, which means extrapolating beyond the data. Mapping DW-MRI data further onto specific microstructural traits is a difficult inverse problem with non-unique solutions, each of which requires strong modeling assumptions. Practical limitations such as the finite voxel size, the finite angular sampling of the diffusion space and, in many cases, the data acquisition limited to a single shell, mean that the information DW-MRI contains about microstructure is far from complete.

### What questions do we ask of the DW-MRI data?

There are, of course, myriad questions that are asked of DW-MRI data – but these can be grouped into classes.

One important class is concerned with the trajectory of fiber pathways and their interpretation in terms of anatomical connectivity, and includes questions of the form: “Which gray matter regions are inter-connected by white matter fibers?”; “Where do these fibers pass?”; and “How strong are these connections?”<sup>4</sup> Usually, the researcher aims to answer such questions by reconstructing continuous longer-range trajectories from local, discrete estimates of fiber orientation. This technique is commonly referred to as tractography (Mori and van Zijl, 2002; Mori et al., 1999; Tournier et al., 2011).

Formally, the fundamental assumption underpinning tractography is that the tangent to the space curve traced by the fiber tract is always and everywhere parallel with the local peak in the orientation density function (ODF) estimated from the data. Moreover, as the local ODF is discretely sampled on the voxel grid, the reconstruction of continuous trajectories from these discrete estimates requires interpolation of the data. Whether a space curve should be propagated as part of the same trajectory at each stage in the iteration process usually involves a rule-based decision involving additional assumptions, for example, on fiber stiffness or maximum curvature. For example, one may set an upper limit on the maximum angle that the trajectory might turn through based on these assumptions (although these thresholds are rarely, if ever, justified in the literature when they are used).

Estimates of fiber orientation are obtained either through the diffusion orientation density function (dODF) or the fiber orientation density function (fODF). The diffusion ODF is a spherical function that, for any point on the sphere, represents the relative number of particles that have diffused along the axis joining that point to the origin. Naturally, this is a symmetric function, since the probability of displacing a mean square distance along axis  $\mathbf{r}$  is identical to that of displacing the same distance along  $-\mathbf{r}$ . With axonal fibers all perfectly aligned along the same axis (i.e., ‘co-axial’) the dODF will be peaked along the long axis of the fibers – and therefore can be used to infer the orientation of the fibers. However, it is important to note that the dODF will be non-zero in all other directions. This is due to the fact that particles can also diffuse perpendicular to the fiber direction (albeit with less ease). Moreover, even if there was no diffusion perpendicular to the fiber, reconstruction from the sampled data would cause the estimated dODF to be blurred (see ‘Modeling of orientation’ section below). Reconstructing the diffusion ODF is the aim of approaches such as diffusion spectrum imaging (Wedeen et al., 2005) and q-ball imaging (Tuch, 2004).

In contrast to the dODF, the fODF is a function that represents the relative number of fibers that are oriented along a given axis. In the case of all fibers being parallel to the x-axis, for example, the true

<sup>4</sup> For a discussion of ‘strength’ of connection and what this might mean, the reader is referred to Jones 2010.

fODF will be a delta function pointing along the x-axis, and zero in all other orientations. Estimated fODFs will of course feature some amount of blurring (see above). Reconstructing the fODF is the aim of approaches such as spherical deconvolution (Alexander, 2005a; Dell'Acqua et al., 2010; Kaden et al., 2007; Patel et al., 2010; Tournier et al., 2004, 2007).

Many tract-reconstruction algorithms exploit peaks in the dODF or fODF to propagate white matter trajectories. Details of different approaches to reconstructing the dODF and fODF will be provided in the section 'Modeling of orientation', below.

A second class of questions asked of DW-MRI concerns the microstructural properties of tissues. Here, questions are asked like: "Where in the brain do we see differences in the local tissue properties between subject or groups of subjects?", "How does disease X or disorder Y affect white matter?", "Does tissue microstructure correlate with task performance?" This type of questions is typically approached by mapping quantities that are derived from local (voxel-wise) models of diffusion. In contrast to the tractography approach, fiber orientation here is not always the most important parameter. Instead, parameters reflecting the total amount of diffusion (apparent diffusion coefficient, ADC) or the diffusion anisotropy (fractional anisotropy, FA) are used (Basser, 1995). These measures are quite sensitive to a number of tissue properties, such as axonal ordering, axonal density, degree of myelination, etc., without being very specific to any one of them. The resulting difficulties in interpretation, along with possible more sophisticated alternatives, are discussed below in the section 'Comparison of microstructural properties'.

We now provide a more detailed appraisal of current approaches to answering these classes of questions.

### Reconstruction of local fiber directions

#### Acquisition: maximum b-factor?

In order to reconstruct longer-range trajectories of white matter fibers, local estimates of fiber orientation derived from the signal are assumed to reflect accurately the true fiber orientation (i.e., be perfectly tangential to the fiber trajectory) as a function of position. This is a very strong assumption that requires several conditions to be met:

- The diffusion time is sufficiently long that water molecules in different compartments of the white matter hit the relevant boundaries;
- The diffusion weighting is sufficiently strong (in terms of duration, temporal separation and amplitude of the gradients), that the size of diffusion-induced signal change is detectable above noise-induced signal variations;
- The sampling of the diffusion signal in time and space is sufficiently dense to reconstruct the ODF; and
- The voxel size is on the order of the spatial extent of the smallest collinear fiber bundles.

With regard to condition (a), the observation of non-monoexponential signal decay has led to the suggestion that diffusing water molecules in nervous tissue fall into at least two distinct populations, having different diffusion coefficients (typically labeled as 'fast' and 'slow') (Clark and Le Bihan, 2000; Clark et al., 2002; Inglis et al., 2001; Maier and Mulkern, 2008; Maier et al., 2004; Mulkern et al., 2001; Ronen et al., 2003). The most common assumption is that the slow component stems from the intra-axonal water where diffusion is restricted (the mean-square displacement becomes independent of the diffusion time as the diffusion time increases) perpendicular to the long axis of the axon and therefore shows a high degree of orientation dependency. The faster component originates from the extra-axonal space where diffusion is just hindered (the mean-square displacement, although lower than in free water, increases linearly with the diffusion time according to the Einstein equation), and is less orientation dependent (Cohen and Assaf, 2002). Diffusion sensitization

at low b-values (e.g.,  $b < 1000 \text{ s mm}^{-2}$ ), leads to almost no signal loss due to the displacement of intra-axonal water perpendicular to the axon.

However, this interpretation of non-monoexponential decay of the diffusion signal is not undisputed. In particular, the experimentally obtained slow and fast diffusion fraction does not agree with extra- and intra-axonal volume fractions as obtained from histology (Grinberg et al., 2011). Different alternative models have been suggested (Kärger et al., 1988; Le Bihan, 2007), but so far none of them has gained general acceptance.

Strong gradients and long diffusion times, resulting in high b-values, lead to complete dephasing and signal loss for the faster moving extra-axonal water (irrespective of the orientation of the applied gradient) and to highly anisotropic signal loss for the intra-axonal compartment (only large components of displacement along the fiber axis will cause the signal to dephase). Hence, higher b-values make the angular diffusion profile sharper and more sensitive to the orientation of fibers. This has been confirmed in simulations (Descoteaux et al., 2009), in which, for example, increasing the b-value from  $1000 \text{ s mm}^{-2}$  to  $3000 \text{ s mm}^{-2}$  reduced the minimal resolvable angle between fiber bundles from about  $45^\circ$  to  $30^\circ$ , while a further increase to  $5000 \text{ s mm}^{-2}$  offered no further improvement. This finding was independent of the number of degrees of freedom in the model (number of spherical harmonics used to represent the fODF) and the number of diffusion-encoding gradient orientations (81 and 321 orientations were tested).

However, increasing the b-value comes with a price tag: one has to remember that DW-MRI is a technique based on signal loss. For a fixed diffusivity, larger b-values mean more signal loss and reduced SNR per unit time. Under the assumption of unlimited gradient hardware capability, this would just mean lower SNR in the diffusion-weighted images. However, since gradient power on clinical systems is limited, increasing the b-value generally means applying the gradients at maximum amplitude – and increasing their duration or temporal separation. In turn, this leads to additional signal loss due to relaxation processes ( $T_1$ ,  $T_2$ ), which will also reduce the SNR in the non-diffusion-weighted images. Hence, one has to find a compromise between SNR and sensitivity of the measurement. So, for resolving peaks in the fiber orientation density, b-values around  $3000 \text{ s mm}^{-2}$  are recommended, if the SNR allows. The simulations of Descoteaux et al. (2009) suggest that an SNR in the diffusion-weighted signal greater than 10 is usually sufficient. The implications of this requirement will be explored in more detail later.

#### Acquisition: How many gradient directions?

Condition (b) involves sampling the diffusion propagator in space and time, that is, for a given orientation, quantifying the relative number of water molecules that have moved a given distance along that orientation within a given time. It is clearly impractical to sample the angular space with arbitrary precision and therefore, the reconstructed fiber orientation distribution will be blurred (with, as discussed above, further blurring imposed by the contributions of the extra-axonal hindered diffusion, especially at lower b-values). This is, of course, not a problem if the fibers are all oriented along the same axis. However, since this is not usually the case – at least in large parts of the white matter (Jeurissen et al., in press) – sampling the diffusion-weighted signal loss along a large number of unique orientations is an important prerequisite for accuracy in the reconstruction of fiber orientation distribution functions. Of course, it would also be a pre-requisite even if, within each voxel, the fibers are all oriented along the same axis, since this axis changes orientation from voxel to voxel. Increasing the number of unique measurements will not only improve the precision (reproducibility) of these reconstructions, but will also reduce the statistical rotational variance, i.e. the extent to which the variance in an estimate of a given parameter depends on the orientation of the structure. For example, with the diffusion tensor model there are only 6 unknown parameters – but it has been shown that for a statistically rotationally-invariant reconstruction (such that the variance in tensor-derived parameters is independent of the orientation of

the tensor) at least 30 directions uniformly distributed over the sphere are needed (Jones, 2004).

Alternative models to the tensor pose different requirements on the number of directions. For example, Tournier et al. (2009) have shown that full characterization of the fODF in white matter using a spherical harmonic deconvolution approach (Tournier et al., 2004, 2007) requires spherical harmonics up to order 8, which requires estimation of 45 coefficients. However, if we only collect 45 measurements – and perform a straight regression – then we will fit to the data *exactly* and therefore also fit to the noise. [Note, however, that several data fitting approaches add a regularization step to the fitting procedure (Descoteaux et al., 2006; Sakaie and Lowe, 2007; Tournier et al., 2004), aiming to ameliorate the effect of noise, somewhat.] More data points allow for a regression, which will reduce the effects of noise. However, the number of unique orientations needed to ensure statistical rotational invariance is, as yet, unknown. It is therefore likely that far more than 45 directions are needed to ensure rotational invariance in the precision of estimates of the peaks in the fODF. Moreover, in the absence of *a priori* knowledge of the orientations of the structures of interest, it is important to distribute these sampling vectors such that they cover the unit sphere as uniformly as possible (White and Dale, 2009).

With hardware currently provided by the major vendors, (gradient amplitudes between 40 and 80 mT/m), and typical image resolution (*i.e.* voxel dimensions on the order of 1.5–2.5 isotropic mm), collecting a whole brain volume takes on the order of 10–15 s (depending on whether or not the acquisition is cardiac-gated). Consequently, it is typically possible to sample the diffusion-weighted signal along 40–60 sampling orientations in 15–30 min. Thus, the requirement to sample diffusion along at least 30 unique orientations to obtain robust estimates of tensor-derived properties (trace, fractional anisotropy and principal eigenvector orientation; see next section) can be satisfied in a reasonable scan time. Note that recent development of simultaneous image refocusing approaches (multiband) (Larkman et al., 2001; Breuer et al., 2005; Sefton et al., 2012; Feinberg et al., 2002, 2010) and compressed sensing approaches (Donoho et al., 2006; Lustig et al., 2007; Doneva et al., 2010; Landman et al., 2010; Landman et al., 2012; Menzel et al., 2011; Michailovich and Rathi, 2010; Michailovich et al., 2011) have huge potential for drastically reducing acquisition times, making the requirement to collect such numbers of gradient directions a clinical reality. More in-depth treatment of the issue of angular resolution can be found in, for example, Alexander (2005b), Jones (2010a), and Tournier et al. (2011).

While discussing ways of optimizing the data acquisition strategy for robust estimates of tensor-derived properties, we note that while vendors have started to provide multiple-orientation sampling schemes for diffusion tensor imaging (*e.g.* 30-direction sampling schemes), the post-processing software most often employs a simple ordinary linear least squares (OLLS) regression to a tensor model, where the signal intensities are log-transformed prior to the model fitting. However, the logarithmic transformation distorts the variances on the diffusion-weighted signals, and thus the assumption of *homoscedasticity* which is implicit in the OLLS approach is invalid. Weighted-linear least squares (WLLS) approaches apply an appropriate scaling to the variances of the data, that accounts for the log transformation (Basser et al., 1994a). Non-linear least squares (NLLS) approaches do not require the logarithmic transform, and therefore make less assumptions about the uncertainty on the fitted data. Koay et al. (2006) have shown in simulations that NLLS outperforms WLLS which in turn outperforms OLLS, in terms of the mean squared error between estimated FA, and 'gold truth' FA, in noisy data. Despite this, the most widely used regression routine is OLLS. As laid out above, this is a suboptimal approach to estimating the tensor and its indices, and WLLS should be used at the least.

The robustness of tensor-derived estimates can be improved even further through the identification and rejection of outliers in the data. Chang et al. (2005, 2012) have shown how automated examination of residuals, in combination with a robust estimator, can allow one to

identify outliers in the data, and reject them. The 'Robust Estimation of Tensors by Outlier Rejection' (RESTORE) algorithm has been shown to provide even more robust estimates of diffusion parameters than standard NLLS. Although there is a time penalty in the regression, it is our opinion that such approaches should be the method of choice when dealing with 'real world' data that are likely to contain outliers.

#### Acquisition: spatial resolution?

Condition (c) points to the other crucial limitation – the finite voxel size. When the dimensions of the voxel exceed that of the dimensions of a fiber population (by population, we refer to a bundle of axons that follow the same course), or, if the voxel lies at the interface of two bundles with different orientations (partial voluming), then ambiguity is introduced – both in terms of location of those populations within the voxel and in terms of their topology.

The signal does not provide any information on the *relative* position of different fiber populations within the voxel. For example, the diffusion-weighted signals from two bundles of fibers arranged in a letter 'T' configuration, a letter 'L' configuration and a '+' sign configuration will be identical (see Fig. 1). Although the 'rotated W' configuration is unlikely to be encountered in the brain, we include it here as an extreme case to illustrate the point that the reconstructed ODF contains no information about the spatial position of fibers aligned along different orientations, and that although the ODF for this configuration would also be a 'cross', this does not mean that the underlying fiber configuration forms a cross shape. We can only 'listen' to what comes out of the 'black box' that is the voxel (see also Kaden et al., 2007, Fig. 2). It is for this same reason, *i.e.* that we have no access to the actual fiber pathways within each voxel, that it is typically very difficult to distinguish between 'kissing' and 'crossing' fiber configurations.

The resolution constraint is a clear limitation in brain connectivity studies – where it is not just the major 'stem' of the white matter pathway that is important – but equally crucial is the ability to identify the insertion points into the cortex. Clearly, however, due to the aforementioned partial volume effects, determining where and how the fibers enter the cortex is a difficult problem for diffusion MR methods, especially for those deployed on a clinical scanner.

Consequently, increasing the spatial resolution as much as possible is crucial, in order to minimize the number of voxels containing multiple fiber populations. However, we can perform a simple thought experiment to get a handle on the resolution that would be needed to achieve this. Of course, avoiding having an interface between different fiber populations within all voxels would be impossible. However, in our thought experiment, we can try to minimize the total number of voxels in the brain in which an interface is found. To do this, we have to make the resolution so high that the probability that each voxel contains just one fiber bundle is high. If coherent units within the white matter measure, say, 100  $\mu\text{m}$ , then a voxel size of 1  $\mu\text{m}$  would be needed to make sure that 99% of the voxels do not contain an interface. Such a resolution is of course unrealistic (and even more astronomic resolutions would be required for resolving single axons), not only due to current hardware limitations, but also because the resulting SNR would be so low that the resulting data would be completely unreliable. Moreover, the spins that give rise to the MR signal would diffuse out of the voxel during the time-scale of the experiment. Currently, the achievable resolution is just below 1 mm (*e.g.*, Heidemann et al., *in press*). As a consequence, multiple fiber populations have to be expected in a substantial portion of the voxels in any realistic setting.

So, even if the ultimate spatial resolution appears unachievable, what prevents us from at least pushing the resolution substantially further in that direction? In general, one has to bear in mind that the signal-to-noise ratio (SNR) depends linearly on the voxel volume. For example, reducing the edge length from 2 to 1.5 mm reduces the SNR by more than half. While it is tempting to think that this reduction

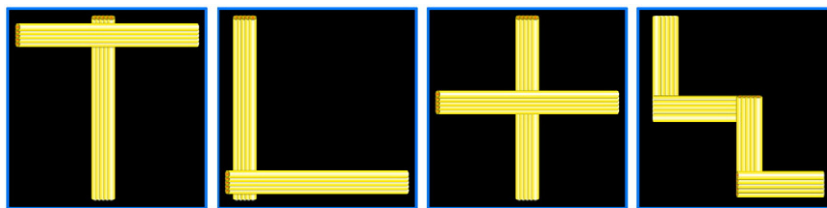


**Fig. 1.** Schematic demonstration of diffusion MRI's insensitivity to *relative* position of different fiber populations in the voxel. Four fiber configurations are shown (T, L, + and rotated 'W'). Despite the fiber populations having entirely different configurations in the different voxels, the fiber orientational density function would be *identical*.

in SNR can be compensated for by repeating and averaging the measurements, it is important to remember that, unless averaging is performed in the complex domain [with associated requirements for careful phase navigation (Anderson and Gore, 1994; Bammer et al., 1999; Butts et al., 1996, 1997)] and appropriate models of the noise are invoked (Aja-Fernández et al., 2008; Brion et al., 2011; Clarke et al., 2008; Dietrich et al., 2008; Koay et al., 2009; Kristoffersen, 2009; Tristán-Vega et al., 2012; Wiest-Daessle et al., 2008) (as discussed below), what is important is the SNR in the diffusion-weighted images. More specifically, the SNR should never be below about 3:1 in any of the diffusion-weighted images – so as to avoid the problems associated with the rectified noise floor (Jones and Basser, 2004) and, as stated earlier, Descoteaux et al. (2009) suggest 10:1 as a safe minimum.

To assess the practical implications imposed by this requirement, we must consider the maximal signal attenuation that may be encountered due to diffusion. First, at higher  $b$ -values, the signal from the Gaussian part of the diffusion-weighted signal is completely attenuated – and therefore we need only consider the signal from the intra-axonal space. The largest diffusivity is found along the long axis of the fiber – which is on the order of  $1 \times 10^{-3} \text{ mm}^2 \text{ s}^{-1}$ . For a given  $b$ -value, the signal attenuation is given by  $\exp(-b \cdot D)$  – and therefore for  $b = 1000$ , 2000 and  $3000 \text{ smm}^{-2}$ , the signal attenuation is  $\exp(-1) = 0.37$ ,  $\exp(-2) = .14$ , and  $\exp(-3) = .05$ , respectively. Thus – when  $b = 3000 \text{ smm}^{-2}$  for example, the diffusion-weighted signal is only 5% of that in the non-diffusion-weighted signal. Therefore, if we adhere to the recommendations that the SNR in the DW-images never drops below 10:1, then for  $b$ -values of  $1000 \text{ smm}^{-2}$ ,  $2000 \text{ smm}^{-2}$  and  $3000 \text{ smm}^{-2}$ , the non-diffusion-weighted SNR must be  $(10/0.37) = 27:1$ ,  $(10/0.14) = 71:1$ , and  $(10/0.05) = 200:1$ , respectively.

However, obtaining SNRs as high as 200:1 can be challenging. The SNR that is achievable is a complex function of the maximum gradient amplitude (since stronger gradients mean that a shorter echo time can be used for the same amount of diffusion-weighting, and therefore  $T_2$ -related signal losses are reduced), the field strength, and the design of the receiver coil (proximity to the tissue being imaged), and the coil loading factor,  $g$ -factor for parallel imaging, and the total number of channels).

As alluded to earlier, strictly speaking this assumes that all images are single-shot. It is possible to average DW-MRI images to improve SNR – but this requires averaging in the complex domain which, in turn, requires complex phase navigation and is not a feature normally provided by hardware vendors.

When selecting the acquisition parameters, one should strive for isotropic resolution since different in-plane and between-plane resolutions would lead to differential averaging of fiber orientations, leading to complicated modeling requirements if this is to be accounted for. With certain MR scanner manufacturers, spatial-spectral pulses are employed to suppress the signal from fat while exciting the desired slice. Current designs impose limitations on the minimal achievable slice thickness – which, if isotropic resolution is used, imposes limitations on the resolution. Ultimately, we recommend selecting the slice thickness and acquisition matrix to ensure that: (a) the resolution is isotropic; and (b) the signal-to-noise ratio in the non-diffusion weighted images is at least as large as  $3/\exp(-b \times 10^{-3})$ , where  $b$  is the  $b$ -value in  $\text{mm}^2 \text{ s}^{-1}$ .

We stress that all of our discussion relating to SNR and our recommendations are aimed at the vast majority of users that take off-the-shelf software packages which take, as their input, magnitude reconstructed diffusion-weighted signals and which inherently assume (albeit often implicitly) that the data have a Gaussian distribution. However, this is generally only true for when a single receive coil is used, and the SNR is above about 3:1 (Gudbjartsson and Patz, 1995; Henkelman, 1985). However, due to the magnitude reconstruction, the signal reconstructed for a single coil has a Rician distribution (Gudbjartsson and Patz, 1995; Henkelman, 1985). Moreover, when signals from multiple coils are combined (as in parallel imaging, for example), then the data have a non-central chi distribution (Brion et al., 2011; Dietrich et al., 2008). Over the last 3–4 years, great strides have been made in correcting for the non-Gaussian distribution of the data, with more appropriate models of the noise. In such situations, one can 'break the noise floor' (Koay et al., 2009) and in this case, the strict requirements to have  $\text{SNR} > 3:1$  in all images can be relaxed. Currently, however, such models and processing steps are not widely available, and so have not been generally adopted. We also stress, that this figure represents an absolute bare minimum SNR, so as to avoid the noise-floor. However, a whole host of other considerations will impact on the minimal SNR required. For example, as the complexity of the model increases (e.g. the order of the spherical harmonic series is pushed higher), the SNR of the experiment should increase accordingly. Here, model parsimony testing can be used to ensure that the SNR of the experiment supports the complexity of the model that one wishes to use (e.g. Alexander et al., 2002; Freidlin et al., 2007; Jeurissen et al., in press). Alternatively, for tractography-based applications, in which successive estimates of fiber orientation are integrated to form a continuous trajectory, minimizing the variance in estimates of fiber orientation at each point is clearly important. Here bootstrapping of the data, using either the repeated samples bootstrap (Jones, 2003; Jones and Pierpaoli, 2005a; Pajevic and Basser, 2003), residual bootstrap (Chung et al., 2006; Haroon et al., 2009), or wild bootstrap (Jones, 2008; Whitcher et al., 2008) would yield invaluable insights into the expected precision in parameter estimates for a given SNR, allowing the user to decide whether the SNR is sufficient for their purposes.

In summary, the data provide orientation and location smoothed maps of the hindrance diffusing particles experienced within a certain distance. We recommend use of the highest possible resolution – but with two constraints: (i) the voxel dimensions should be isotropic; and (ii) unless appropriate models for the noise distribution are included in the analysis (Aja-Fernández et al., 2008; Brion et al., 2011; Clarke et al., 2008; Dietrich et al., 2008; Koay et al., 2009; Kristoffersen, 2009; Tristán-Vega et al., 2012; Wiest-Daessle et al., 2008) the SNR in the diffusion weighted images should not fall below 3:1. However, this is a bare minimum and, depending on the model complexity/application, the SNR may need to be much higher. Current state of the art, with single-shot methods, dictates an isotropic voxel size on the order of 1.5–2 mm at a static field strength of 3 T.

Currently, with the hardware and software typically provided by the major vendors, it can be recommended to sample about 60–80 optimally distributed gradient directions, use a  $b$ -value of at least  $1000 \text{ smm}^{-2}$ , better  $2000\text{--}3000 \text{ smm}^{-2}$ , and keep the SNR in all images safely above 3:1. Parallel imaging (GRAPPA or SENSE) (Griswold

et al., 1999; Griswold et al., 2002; Pruessmann et al., 1999) is one established way to reconcile these requirements with an acceptable acquisition time and should be used whenever possible. Moreover, recent developments such as multiplexing (Feinberg et al., 2010; Reese et al., 2009) and compressed sensing (Donoho et al., 2006; Lustig et al., 2007 (Doneva et al., 2010; Landman et al., 2010, 2012; Menzel et al., 2011; Michailovich and Rathi, 2010; Michailovich et al., 2011), although not widely available yet, will bring the acquisition times down even further.

Using ultra-high field imaging (e.g., 7 T) in conjunction with parallel imaging and reduced field of view has been shown to reduce the isotropic resolution to a little as 800  $\mu\text{m}$  with acceptable orientation resolution and SNR, revealing fine details of the fiber architecture, for example at the gray–white matter interface (Heidemann et al., *in press*). Although these techniques are currently far beyond the capabilities of clinical scanners and the requirements of clinical routine (e.g., in terms of acquisition time), they demonstrate what is technically possible in principle and highlight future possibilities.

Finally, while discussing the impact of resolution, the impact of CSF contamination on diffusion MRI metrics should be discussed. Given that CSF is isotropic and has a mean diffusivity that is approximately 4 times larger than water in tissue, it is clear that any extent of partial volume contamination of the voxel by CSF will bias findings. This is particularly problematic at the interfaces of tissue with CSF-filled spaces (Concha et al., 2005), and will impact on inferences about changes in tissue microstructure during development and aging, and indeed in many pathological processes, where there is a change in tissue volume (Vos et al., 2011). Thus, the acquisition and/or analysis pipeline should strive to ameliorate the impact of CSF contamination.

CSF-suppression techniques, such as FLAIR, have been used to ameliorate CSF-contamination at the point of acquisition (Chou et al., 2005; Papadakis et al., 2002), but we note that their use can prolong acquisition time and preclude the possibility of cardiac-gating of the acquisition, to avoid pulsatility effects (Jones and Pierpaoli, 2005b; Pierpaoli et al., 2003). There have been various methods proposed for correcting for CSF-contamination at the post-processing stage, some more robust than others. We currently recommend the use of a multi-component modeling solution (Pasternak et al., 2009; Pierpaoli and Jones, 2004), over other approaches such as covarying for parenchymal volume. The reader is referred to Metzler-Baddeley et al. (2012) for a discussion on the relative strengths of different approaches. The bottom line is that when examining tissue that interfaces with CSF-filled spaces, particularly when there are pathology/aging/developmental processes occurring, accounting for CSF-contamination is an absolute mandate, in order to draw robust conclusions from the data.

#### Preprocessing of data

Prior to modeling, it is essential that data are examined for artefacts and corrected for both motion and eddy-current induced distortions. Here we issue a word of caution when using off-the-shelf software packages to correct for motion and eddy-currents. Frequently, this is done using a registration package that performs an affine registration of the diffusion-weighted images to one of the non-diffusion-weighted images in the series. While this provides a reasonable correction for motion, it does tend to neglect the fact that eddy-current induced distortions will be slice-specific, but again, performing a global affine registration is far preferable to no correction at all.

However, there are two points that are often overlooked. The first is that when correcting for subject motion, if there is a rotation of the image involved in the image registration, then the same rotation must be applied to the encoding vectors. Neglecting to perform this important step may have minimal impact on scalar indices such as fractional anisotropy, but it can introduce biases of the order of a couple of degrees to estimates of the principal eigenvector, or peaks in the fODF or dODF (Leemans and Jones, 2009). When one considers that reconstructing of a fiber trajectory integrates many estimates of

fiber orientation, the impact of this bias becomes obvious. Therefore, especially as the time-penalty for performing this simple processing step is minimal, we recommend reorientation of the encoding vectors in all preprocessing pipelines. We stress that not all software packages used for preprocessing of diffusion MRI data incorporate this step, and urge the reader to verify what their software package of choice is doing in this regard.

The second issue arises if there is a residual eddy current along the phase-encode direction. Such an eddy current will lead to a stretch/compression of the image along the phase-encode axis in diffusion-weighted EPI images. The MR signal intensity is proportional to the volume of the voxel and thus an eddy current of this type will artefactually reduce/increase the signal intensity. Given that, in keeping with our opening comments of the section What does diffusion-weighted MR imaging actually measure? all that we measure in diffusion MRI is a change in signal intensity, this change in signal would be interpreted as a change in diffusion if not corrected for. It is a trivial step to modulate the signal intensity back to its correct value by scaling the intensity in proportion to the change in the volume of the voxel. Neglecting to do this can again introduce biases in quantitative metrics and estimates of orientation (Jones and Cercignani, 2010). However, again we note that not all software packages commonly used for pre-processing of diffusion-MR data include this step and, again, we note that the time-penalty for performing this step is negligible, so is 'recommended practice'.

We cannot stress enough the importance of eyeballing the raw image data prior to proceeding on to further analyses. Viewing the data as a movie loop, cycling through the different diffusion-weighted volumes, can be an effective way of detecting outliers in the data (such as slice-drop outs), particularly when viewing data reconstructed in the two planes orthogonal to the acquisition plane (e.g. if the data are acquired in the axial plane, slice-drop outs are trivially spotted when viewing the data in the coronal or sagittal planes). Moreover, given that head motion in the scanner tends to be gradual and continuous, the first and last volumes in the series will tend to have the largest misalignment. It is therefore prudent to alternate between the first and last volumes in the series to ensure that the motion correction has been efficient.

Finally, we strongly recommend as a useful tool, to examine the residuals of the fitting procedure as a way of identifying artefacts in the data. Even if the data are subsequently to be analyzed *via* non-tensor methods, examining the residuals to a tensor fit to the data can still be extremely useful in identifying artefacts in the data such as ghosting, motion, slice-drop outs, pulsatility and other perturbations (Jones and Leemans, 2011; Tournier et al., 2011).

#### Modeling of orientation

There are two principal ways to mathematically represent the orientation dependence of the diffusion-weighted MR signal, as discussed in the [Introduction](#): To estimate the diffusion ODF or the fiber ODF (see [Fig. 2](#)).

*Diffusion ODF approaches.* The first class of approaches involves trying to reconstruct the diffusion propagator, *i.e.*, the ensemble-averaged probability density that a particle has moved a certain distance within the diffusion time. In principle, and in the limit of time to acquire data, such approaches seem to confer an advantage over fODF methods – no uncertain model assumptions have to be used. The approach is to simply characterize the diffusion itself. However, in order to make any inferences about the tissue, there is then an implicit modeling – in that assumptions have to be made about the relationship between the diffusion propagator and the tissue microstructure properties (e.g., fiber bundle directions or volume fractions) one is interested in.

In practice, however, exact reconstruction of the full diffusion propagator is not possible – especially with practical acquisition schemes, most commonly employing a single b-value. In such cases, substantial modeling simplifications must be invoked. The most

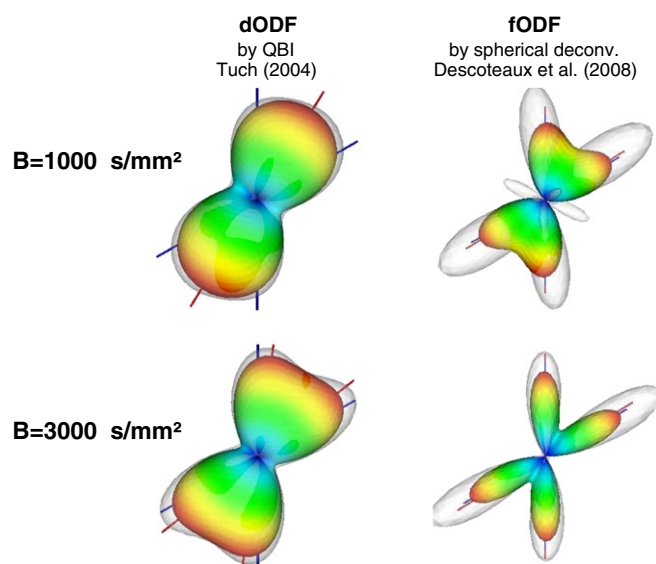


**Fig. 2.** Reconstruction of diffusion and fiber ODFs on the basis of the analytical Q-ball (Descoteaux et al., 2009; Tuch, 2004), computed from synthetic data for two parallel fiber populations crossing at 45°. The colored surface shows the mean fiber orientation density, averaged over 100 noisy trials, while the transparent surface corresponds to the mean + 2 standard deviations. Blue and red lines indicate the ground truth fiber directions and detected maxima, respectively. (For interpretation of the references to color in this figure legend, the reader is referred to the web version of this article.) Modified from Descoteaux et al. (2009).

common such simplification is the assumption of unimodal anisotropic Gaussian diffusion, leading to the diffusion tensor modeling approach (Basser et al., 1994a, 1994b). This approach appears to be a good approximation when the voxel contains only a single co-axial fiber population and a relatively small b-value is used (thus, in a radial orientation, focusing on extra-axonal water – and the first terms of the cumulant expansion). However, as pointed out above, due to practical and SNR-constraints on spatial resolution, many voxels contain multiple fiber populations, bending fibers, and other deviations from the parallel fiber bundle assumption. This issue (generically referred to as the ‘crossing fiber problem’) drove the development of alternative techniques to diffusion tensor MR imaging, which aim to recover more information on the diffusion propagator, and especially its angular portion – the dODF, than obtained from the tensor-modeling approach.

Analytical Q-ball imaging, as proposed by Tuch (2004) as well as Descoteaux et al. (2007), estimates the radial integral of the diffusion propagator using the Funk–Radon transform and therefore resolves multi-modal peaks in the dODF that would be missed by the tensor model. Note, however, that the original formulation of Q-ball imaging fails to account correctly for the differential volume element in spherical coordinates, so the result is somewhat blurred with respect to the correct dODF and lacks proper regularization. Tristán-Vega et al. (2009) as well as Aganj et al. (2010) have presented the correct formulation, also referred to as *constant solid angle* (CSA) Q-ball imaging.

As an alternative to defining the dODF as the radial integral of the diffusion propagator, one might assume the angular distribution of the diffusion propagator to be persistent over all radii, which leads to the definition of a Persistent Angular Structure (PAS) on the unit sphere (Jansons and Alexander, 2003). The PAS is determined in such a way that the resulting diffusion propagator has minimum information content (maximum entropy) compared to a diffusion propagator with no angular structure at all, under the constraint of the data. A similar approach has been proposed by Özarslan et al. (2006) who compute a Diffusion Orientation Transform by expressing the inverted Fourier integral by a Raleigh expansion assuming

mono-exponential radial decay of the signal, and evaluating the integral at a particular radius.

The second principal approach for describing the dODF comprises modeling the signal attenuation as coming from distinct sub-components of the tissue, each of which can be accounted for by a relatively simple model. This leads to the idea of multi-compartment models. For example, if one assumes that within a voxel there are two or more relatively coherent fiber populations with different orientations, one may extend the simple tensor model by summing up the contributions of multiple tensors (Liu et al., 2004; Tuch et al., 2002). A similar approach has been proposed by Behrens et al. (2003) – they used an isotropic compartment (ball: “round” tensor with all eigenvalues equal) and one or several anisotropic compartments (sticks: “thin” tensors with only one non-zero eigenvalue). An important question in compartment models is that of model complexity, *i.e.*, how many compartments (tensors, sticks) one should use to explain the data. This problem can be tackled using model selection procedures (*e.g.*, Behrens et al., 2007; Freidlin et al., 2007). Assaf and Basser (Assaf and Basser, 2005; Assaf et al., 2004) proposed a framework combining elements of diffusion tensor and Q-space imaging, the Composite Hindered and Restricted Model of Diffusion (CHARMED). The model consists of two parts, accounting for hindered diffusion in the extracellular space and within cell bodies (*e.g.* oligodendroglia) and for restricted diffusion in the intra-axonal space, respectively. Hindered diffusion is modeled by a diffusion tensor, while restricted diffusion requires special solutions for a cylindrical restricted diffusion space. The parameters of the model, including the respective volume fractions of the compartments and the principal diffusion directions need to be estimated from measurements at both low and high b-values.

*Fiber ODF approaches.* In contrast to diffusion propagator and dODF approaches, which essentially describe the diffusion within a voxel, fiber ODF techniques aim at estimating relative fiber density over orientation space. This requires specific model assumptions on the diffusion or the signal attenuation caused by a single fiber. More specifically, one tries to infer only the angular distribution of fiber orientations from the angular structure of either the signal (Tournier et al., 2004, 2007) or of the dODF (Descoteaux et al., 2009) by spherical deconvolution with a kernel. This kernel is essentially the simplest model of the diffusion properties of a single fiber that the data support. The deconvolution kernel is obtained either by assuming that white matter with the highest anisotropy must contain a single fiber orientation, or by simulating the response for an idealized fiber.

Clearly, the axon diameter, packing density, membrane permeability and other aspects of the white matter may vary from brain region to brain region – and thus the ‘single fiber response’ will only be an approximation that is generalized across the brain. However, despite this modeling assumption, it appears that fODFs are superior to dODFs with respect to angular resolution and precision (see, for example, Descoteaux et al., 2009). This class of techniques must currently be viewed as sharpening of the angular diffusion profile (Descoteaux et al., 2009) rather than an exact quantification of the fiber orientation profile. Due to the spatial high-pass filtering property of the deconvolution process, these methods are somewhat sensitive to correct regularization, in order to prevent spurious features in the fODF (Tournier et al., 2007).

Interesting variants include the iterative damped Richardson–Lucy approach of Dell’Acqua et al. (2010) and the deconvolution of the diffusion ODF rather than the data (Descoteaux et al., 2009). With this latter method, the dODF (q-ball) and fODF can be compared directly. While both QBI and spherical harmonic deconvolution according to Tournier and Descoteaux rely on a rather cumbersome parameterization (through the coefficients of spherical harmonics), more convenient parameterizations (which directly yield interesting values like the main directions and angular spreads of fiber bundles) are offered by

compartment models (e.g., Behrens et al., 2003; Liu et al., 2004) and by the parametric spherical deconvolution technique (Kaden et al., 2007).

It is important to note that the information encoded in the local model about the orientational spread or incoherency within a given fiber population is heavily confounded with uncertainty about the orientation of the fiber bundle itself. Such uncertainty arises from multiple sources including: noise (Jones, 2003) and the model regularization it necessitates; incomplete modeling of the different diffusion compartments; and the limited angular and spatial sampling.

In summary, for reconstructing the local fiber orientations with reasonable accuracy, it is not only important to measure signal attenuation along a sufficiently large number of unique orientations, but also to model the data in a way that preserves this orientation-dependent information. Thus, in all cases when the voxel contains more than one fiber population, the diffusion tensor model is inadequate for this purpose.

Before moving on to describing the reconstruction of fiber pathways, we do wish to make a point very clear. The majority of deconvolution procedures were designed primarily as pre-processing for fiber tracking, where the diffusion characteristics for a single fiber orientation are deconvolved from the fODF. As a consequence, the fODF is used to infer on the relative number of fibers aligned with a particular axis. This results in sharper reconstruction of the fiber orientation in comparison with the dODF. It should be noted that deconvolution approaches most often assume a canonical single fiber response. Thus, if there is a change in the diffusion characteristics of an individual fiber (so that it is different from the assumed canonical response), this would be reflected in the reconstructed fODF (Parker and Jones, 2011, 2012). If the kernel used in the deconvolution procedure stays constant, then what we reconstruct reflects some kind of apparent fiber density (Dell'Acqua et al., 2012; Raffelt et al., 2012).

#### Reconstructing fiber pathways

There are a number of algorithms that are designed to combine local discrete (voxel-based) models of fiber orientation (derived from either the principal eigenvector for the diffusion tensor, peaks in the dODF or peaks in the fODF) and reconstruct continuous fiber pathways. These techniques are collectively referred to as *tractography*. It should be emphasized that none of these methods is capable of reconstructing nerve fibers or even fiber bundles. Instead, they compute trajectories or pathways through the data, to which (hopefully) a large portion of the nerve fibers run reasonably in parallel. These pathways are currently interpreted both in a qualitative way, when they are used to infer on the extent and the general course of certain fiber bundles, and in a quantitative way, either as a three-dimensional region of interest (ROI) from which quantitative metrics can be derived (Jones et al., 2005a) or trying to estimate the 'degree of connectedness' between brain regions (e.g., Kaden et al., 2007). The latter issue of quantifying anatomical connectivity from DW-MRI data has been treated systematically and critically in a recent review article by Jones (2010b) which concluded that the orientation information encoded in the fODF/dODF is necessary but *insufficient* for quantifying white matter connections. In addition to obtaining orientation information, further *microstructural* information, which provides characterization of distinct sub-compartments of the white matter, is an absolute necessity.

In contrast, measures derived from the diffusion tensor, such as fractional anisotropy, essentially combine the contributions from the different sub-compartments of white matter into a single metric. Improving the biological specificity of diffusion MRI demands improvements in acquisition schemes (e.g. designed to maximize information on microstructural traits other than fiber orientation). Advanced diffusion MR methods can provide putative axonal markers, such as 'axon density', mean axon diameter and axon diameter distributions [CHARMED (Assaf and Basser, 2005; Assaf et al., 2004), AxCaliber (Assaf et al., 2008), ActiveAx (Alexander et al.,

2010)]. Quantification of myelin *via* diffusion is extremely problematic, and other MR contrast mechanisms such as quantitative magnetization transfer imaging (Cercignani and Alexander, 2006; Sled and Pike, 2001), and multi-component relaxometry (e.g., Deoni et al., 2008; Kolind and Deoni, 2010) hold more promise in providing putative myelin markers.

In addition to considering new contrast mechanisms, there is not only a pressing need to improve analysis methods but also to consider, more carefully, the approaches that are currently in use. For example, one approach to quantifying connectivity between two brain regions involves counting the number of times that a streamline can be reconstructed between them. This can be done in two different ways. On the one hand, one can start tracts at multiple starting points in one or several voxels, using always the same local fiber orientation information, usually derived from modes (principal directions) of the local ODFs. This technique is referred to as *deterministic tractography* (Conturo et al., 1999; Mori and van Zijl, 2002; Mori et al., 1999) and can be used to estimate connectivity by counting the number of fiber pathways starting from or passing through a certain region. On the other hand, one may interpret the local ODF (fiber or diffusion ODF) as a probability density distribution of the local fiber orientation, randomly sample this distribution many times, and perform streamline tractography with each sample from always the same starting point. The technique, usually referred to as *probabilistic tractography* (Behrens et al., 2003; Koch et al., 2002), yields maps that are related to the probability that a certain voxel is connected to the starting point (e.g., Kaden et al., 2007).

The result of both the deterministic and probabilistic approach is often interpreted as 'connection strength'. However, the ability to faithfully follow a white matter trajectory by integrating discrete estimates of its tangent (derived from peaks in the dODF/fODF) depends on the SNR of the experiment (Huang et al., 2004; Lazar and Alexander, 2003; Lori et al., 2002) – which modulates the uncertainty in fiber orientation at each stage of the streamline propagation. It seems strange, therefore, that the connectivity of the brain depends on the parameters of the MR experiment.

#### Can 'fiber count' be determined from DWI data?

As we have previously shown (see Fig. 4 in Jones, 2010b), even if the 'true' fiber count (in terms of number of axonal projections) is uniform within a bundle, the number of reconstructed streamlines in the experiment may be different just because of the length, curvature and degree of branching. Yet, there is no reason to believe that a curved and straight fiber bundle with an identical number of axon projections, would have different capacities to carry information.

Thus, our concern is really about interpreting the number of reconstructed streamlines as a true measurement of the number of actual fibers (axonal projections) as would be identified if the same piece of brain tissue was examined histologically. Moreover, our concern is also on the expectation *a priori* that this should be the *primary* and, in some cases, sole covariate of any measure of function. If all other features of the pathway (curvature, length, width, myelination) and experimental conditions (e.g. local variations in SNR) were kept the same so that the only thing that differed was the number of axonal projections, then one might reasonably expect the number of reconstructed streamlines to be a good indicator of the number of 'fibers'. However, as noted above, there are many other reasons why the streamline count may vary. Thus, we would strongly discourage the use of the term 'fiber count'. Rather, we propose that reporting of the number of reconstructed streamlines *i.e.*, 'streamline count' is a far safer and unambiguous way of reporting results. It indicates that there is a dependence on the tractography algorithm and the experimental conditions.

For the same reason, the number of streamlines passing through a given voxel will also be modulated by the same factors – so that interpreting this measure as 'fiber density', as is done in the literature,

introduces equally challenging problems for interpretation of results. To the best of our knowledge, there is no method extant to correct for the kinds of problems related to tract length, curvature and branching described elsewhere (Jones, 2010b). Despite these confounding effects of length, curvature and branching, the use of ‘fiber count’ and similar metrics/terminology has, nevertheless, increased. They are used in graph theoretical approaches and in mapping the ‘connectome’ (Hagmann et al., 2007, 2008, 2010; Honey et al., 2009). However, assigning a ‘connection strength’ between two cortical nodes, without accounting for these (non-interesting) topological sources of variance in such metrics, is fraught with danger for robust interpretation. In other words, although, from a Bayesian point of view, these connectivity values are the best possible guesses (in the absence of any further information), what is not apparent from any of these studies is the huge uncertainty (variances) attached to them. Methods need to be developed that compensate for differences in both length and shape of tracts. Until such time as these methods are developed, it may be dangerous to compare even the streamline count in white matter structures that have different shapes.

It is important also to note that here the term ‘probabilistic’ in the context of tractography suggests, somewhat misleadingly, that the analysis pipeline yields some kind of formal probability that voxels are actually connected by white matter fibers. It is not uncommon to hear an interpretation that probabilistic tracking algorithms yield a ‘probability of an anatomical connection’. We would like to spend a moment considering what this might actually mean, and suggest that the end-user might wish it to mean something similar to the following:

“If I look at a probabilistic tracking map where I have launched tracking from a point X, the result tells me how confident I can be that if I was to open up the brain and look directly at the white matter, where the map intensity is high, I am more likely to find an actually white matter pathway that travels back to the point X, compared to the case when the intensity is low.”

However, while this is not completely incorrect, one has to consider three important issues. First, it is not clear what the existence of a connection between two brain regions A and B actually means: if it means that at least one axon runs between A and B, then the probabilities would be almost always close to one, if it means that all axons starting in A end in B (or *vice versa*), the probability would be zero. Both values are clearly useless. Therefore, the most sensible thing to do is to use a probability distribution, stating how probable it is that the connection strength (*i.e.*, the number of axons) exceeds a certain value. This would require disentangling the connection strength and the probability thereof from tractography data, which is a severe challenge, to say the very least. See also Kaden et al. (2007).

Second, although it may be fair to assume a monotonic relationship between connection probability (whatever it may be, see above) and probabilistic tractography score, there is no exact quantitative equivalence between the two. This would require a much more detailed and formalized description of the whole chain of measurement and analysis processes.

Third, tractography can only estimate a marginal probability. The tractography score simply indicates how frequently we can reconstruct a streamline from a particular point, or between two points, in the brain, and there are many reasons why a streamline may not be successfully reconstructed (Jones, 2010b), differences in true ‘connection strength’ are just but one.

To date, no method has been proposed that yields a true statistical probability, and so although the ‘probabilistic’ adjective has been adopted now, a more appropriate adjective would be ‘stochastic’ tractography. While it is fair to take an enhanced probabilistic tractography score (cautiously!) as an indication for increased connectivity, one should (1) not interpret it literally as a probability

(*e.g.*, for use in statistical tests) and (2) be aware it could also be caused by other factors (and that these biases are by far not small or uncommon).

Finally, the reader should not infer that we are ‘throwing the baby out with the bath water’ here. Rather, our comment is on quantitative assessment of connectivity derived from diffusion MRI. Without question, impressive and useful *qualitative* results on the shape of fiber bundles and the connection patterns of brain regions have been achieved by just exploiting the orientation information contained in the diffusion-weighted MR signal. However, while the orientation information contains important information on brain connectivity, it is insufficient for its complete characterization.

#### Comparison of microstructural properties

The sensitivity of DW-MRI to local (microstructural) tissue properties renders the technique a powerful instrument for the investigation of anatomical correlates of numerous experimental and clinical conditions. The extent to which the random displacement of water molecules is impeded in any direction will be dependent on numerous factors that are of functional relevance including, but not limited to, the fiber diameter, fiber density, membrane permeability, and myelination – in *addition* to the intra-voxel orientational coherence of any boundaries (Beaulieu, 2002).

Changes in these various tissue properties may be associated with disease, development, learning, *etc.* Consequently, there have been a large number of studies in recent years correlating differences in various DW-MRI derived measures between experimental conditions (*e.g.*, before and after learning or training) or subject groups (*e.g.*, patients and healthy controls). For example, DWI data of patients with Alzheimer's disease (Avants et al., 2010; Damoiseaux et al., 2009; Gold et al., 2010; Jahng et al., 2011; Mielke et al., 2009), autism (Cheng et al., 2010; Fletcher et al., 2010; Pugliese et al., 2009), schizophrenia (Jones et al., 2005b, 2005c; Qiu et al., 2009, 2010), mild cognitive impairment (Jahng et al., 2011), multiple sclerosis (Bodini et al., 2009; Roosendaal et al., 2009), amyotrophic lateral sclerosis (Ciccarelli et al., 2009; Iwata et al., 2011), Tourette's syndrome (Neuner et al., 2010), Parkinson's disease (Menke et al., 2009), and Huntington's disease (Rosas et al., 2010) have been compared to healthy controls. Moreover, the effects of aging (Davis et al., 2009; Michielse et al., 2010; Moseley, 2002; Pfefferbaum et al., 2005; Sullivan and Pfefferbaum, 2006), development (Faria et al., 2010; Goodlett et al., 2009; Kochunov et al., 2009), learning (Flöel et al., 2009; Lebel et al., 2010) and intellectual performance (Liu et al., 2010; Lee et al., 2010) were investigated. For a recent review of studies on the behavioral relevance of white matter microstructure as quantified by diffusion MRI, see Johansen-Berg (2010) and Kanai and Rees (2011).

In almost all of these studies, the DW-MR data were modeled by a diffusion tensor. Scalar measures, like fractional anisotropy (FA), mean diffusivity (MD), radial and axial diffusivity (RD, AD) (Basser, 1995; Song et al., 2002) were then computed and mapped – and compared either by using manually drawn regions of interest (ROIs), by sampling the parameters of interest along a tractographically reconstructed pathway (Jones et al., 2005a) comparison of whole brain histograms, or *via* voxel-based search methods. The reader is referred to Cercignani (2010) for an in-depth exploration of the relative strengths and weaknesses of each method. An interesting discussion in the light of white matter degeneration in Alzheimer's disease can also be found in Acosta-Cabronero et al. (2010).

Changes or differences in these measures are often interpreted as changes or differences in the “integrity” of the white matter microstructure (or, in the opposite way, as structural damage, decline or degeneration). This implies that some aspect of the white matter microstructure is damaged. While in disease and aging-related studies, such an interpretation can be often justified, the term “integrity”

seems to be misplaced when used in the context of FA changes related to, e.g., learning success (Flöel et al., 2009), intelligence (Liu et al., 2010) or creativity (Takeuchi et al., 2010).

There is no doubt that that the presence of a difference in the diffusion-weighted signals between two or more groups of subjects, or a correlation between a metric derived from those signals and a behavioral measure, is a useful outcome, if and only if it is proven to be robust, reliable and reproducible. The dangers come when trying to interpret these differences. Given the degenerate nature of the contribution of different microstructural features to variations in signal dephasing, it is pure fallacy to assert that a particular aspect of the microstructure is likely to be responsible for the signal difference. For example, it is not uncommon for researchers to have found a difference in the anisotropy of the fitted diffusion tensor between two groups – and then to say something like ‘and this probably reflects differences in myelination’. The anisotropy in a region may also be lower because there is a larger axon diameter (Takahashi et al., 2002), a lower packing density (Takahashi et al., 2002) – both of which mean fewer barriers to diffusion in a given space – or it could be due to increased membrane permeability (reducing the effectiveness of a boundary).

Perhaps because of these multiple possible sources for the differences in the diffusion-weighted MRI signal, the rather vague terms ‘white matter integrity’ and ‘microstructural integrity’ have become popular in the literature. While one can see the motivation for invoking such terms, their use really should be discouraged and discontinued. In English common usage, a loss of ‘integrity’ is a serious problem. For example, if there is a transient change in the permeability of the axonal membrane – is the microstructural ‘integrity’ of the system really reduced? Moreover – and most importantly – as demonstrated by Pierpaoli and Basser (Pierpaoli et al., 1996) over a decade ago, the most important determinant of the anisotropy of a uni-modal Gaussian tensor fitted to the data is the ‘architectural paradigm’ – i.e., exactly how the subunits (axons) are laid out in the voxel. It is a trivial mind-experiment to consider two voxels, A and B, in the white matter, each comprising  $N$  fibers. In both voxels, the axon diameter, membrane permeability and myelination of each axon is the same. So – at the ultra-structural level, the ‘integrity’ of each axon is identical. However, in voxel A, all the axons are aligned along the same axis and densely packed, while in voxel B – the axons are much less coherently organized – with a range of orientations (such as might arise from fibers fanning, branching, crossing, twisting). The anisotropy of the tensor fitted to voxel A will be much higher than that of voxel B – but it would be a complete fallacy to argue that the microstructural integrity was lower in voxel B. Yet – this sort of logic is routinely applied in the interpretation of DW-MRI data in the literature. Such imprecise and potentially misleading terminology is unhelpful for scientific understanding.

To take a further example: as the brain develops, and more connections are formed, so that the intra-voxel orientational coherence is reduced, with a concomitant reduction in diffusion anisotropy, should we infer that brain maturation entails a loss of white matter integrity? For a particular ‘DON’T’ – we stress ‘DON’T’ blindly interpret changes in the diffusion-weighted MR signal as a change in microstructural integrity!

It is also important to note that FA is a local metric that is derived just for the water molecules confined within the image voxel. Thus, inferring on a connection (which typically occurs over a larger scale-length), and therefore on connectivity, is extremely problematic. Moreover, FA is modulated by the intra-voxel orientational dispersion, the myelination, the packing density, membrane permeability, and partial volume effects in addition to the number of axons. Thus, a change/difference in FA most probably reflects some changes/differences in some aspects of connectivity, although we cannot really say what precise aspect, and into which direction the change. Thus, one can see that any notion of being able to relate the voxel-derived FA metric in a linear fashion to ‘connectivity’, such that, for example, low FA = low connectivity, high FA = high

connectivity, is completely flawed, and thus we stress ‘DON’T’ blindly interpret changes in anisotropy as a change in connectivity in any quantitative way!’

Independently of the appropriateness of the term “integrity”, the actual meaning of the tensor-derived measures is extremely ambiguous. The tensor is usually described by its eigenstructure, comprising eigenvectors and eigenvalues. As pointed out above, under the conditions of reasonably parallel fibers throughout the voxel and in the low- $b$ -value regime, the single diffusion tensor model is adequate. In this scenario the eigenvector associated with the largest (principal) eigenvalue indicates the main fiber orientation, while the principal eigenvalue, often referred to as axial diffusivity (AD), describes the water mobility along this axis and the other two eigenvalues, referred to as radial diffusivity (RD), should be similar and reflect water mobility perpendicular to the fiber axis. The relationship between AD and RD (degree of anisotropy) can then be expressed by measures such as fractional anisotropy (FA), which denotes the ratio of standard deviation and root mean square of the eigenvalues. It is clear that in such a situation, increasing axonal density, reducing axonal caliber and increasing the degree of myelination should all lead to reduced RD and therefore elevated FA.

Indeed, it has been convincingly demonstrated in eight different fiber tracts in shiverer mice that myelin loss alone (without loss or degeneration of axons) can cause an increase in RD, while the AD remains unchanged (Song et al., 2002), see also Roosendaal et al. (2009) and Stricker et al. (2009). It was argued that, in contrast, axonal loss would not have affected RD. This argument was based on the assumption, put forward by earlier researchers (Klingberg et al., 1999; Wimberger et al., 1995), that the effect of myelin on the RD is due to hindrance of transmembrane water transport by the myelin sheath. It is not clear whether this transmembrane transport really has an impact on water diffusion at the timescales considered here. According to Assaf and Cohen (2000) the signal modeled by the diffusion tensor depends mainly on extra-axonal diffusion for the small  $b$ -values considered. An alternative explanation is that myelin loss opens extracellular spaces (see, e.g., Fig. 2 in Song et al., 2002), allowing for more free diffusion perpendicular to the main fiber direction. However, the same effect would then be observed for axonal loss. Hence, an increase in RD at low  $b$ -values can have multiple meanings, including myelin loss and loss of axons.<sup>5</sup>

However, as has been emphasized above, the assumption that white matter fibers run parallel within a voxel often does not hold in general, especially in the human brain, with differing reports in the literature on the amount of complexity present.

The exact number of voxels that are deemed to contain more than one fiber populations will obviously depend on the data quality, the model and the analysis pipeline used. The angular resolution of the sampling scheme, together with the  $b$ -value and the SNR will impact on the minimum resolvable inter-fiber angle and, therefore, the number of distinct fiber voxels that can be identified within a voxel. For example, Behrens et al. (2007) only found that one third of voxels contain 2 fiber populations. Jeurissen et al. (in press), however, using more extensive data acquisition and alternative modeling technique estimate the proportion of WM voxels containing crossing fibers to be approximately 90%, using constrained spherical harmonic deconvolution, and 63% when using the automatic relevance detection approach of Behrens et al. (Cohen and Assaf, 2002).

Of course, the likelihood of finding any voxels in which all axons within that voxel are perfectly co-axial is exceedingly unlikely. Thus, even a ‘spreading’ could ultimately be resolved into multiple fiber populations and so, as the techniques improve even further, all white

<sup>5</sup> In spite of this objective lack of specificity, tensor derived measures are often endowed with quite specific interpretations. For example, increase in RD has been interpreted as reflection of demyelination due to HIV (Chen et al., 2009) or reduced myelination during development (Cykowski et al., 2010).

matter voxels could ultimately be deemed to contain ‘crossing fibers’. While this will be ameliorated by moving to higher resolution acquisitions, again – it is unlikely that many voxels will contain axons that have a single orientation.

In such situations, RD and AD are additionally influenced by the orientation spread of the fibers. The tensor model then effectively becomes completely meaningless, when more than one principal orientation is present in a voxel, e.g., at fiber bundle crossings (Wheeler-Kingshott and Cercignani, 2009). Note that this situation affects between one and two thirds of the voxels in the human brain (Behrens et al., 2007; Descoteaux, 2008; Jeurissen et al., 2010).

Consequently, in the majority of voxels of a brain DT-MRI data set it is very difficult to interpret observed differences or changes in tensor derived measures in terms of a specific microstructural attribute. For example, a decrease of MD and RD (and the associated increase in FA) in the Arcuate fascicle as found in high functioning autism (Fletcher et al., 2010) could be due to a more coherent alignment of fibers in the Arcuate, fewer crossing fibers from other bundles, higher density or stronger myelination of the Arcuate fibers, or even a loss of certain axonal fibers within the Arcuate, resulting in the remainder being more coherently organized, or a combination of any, or all, of these factors.

Part of the ambiguity in the interpretation of differences in DW-MRI derived measures is rooted in the measurements themselves. Limited spatial and angular resolution as well as the restriction to a single or a few b-values limit the information content of the data. However, this ambiguity is further increased by the use of the diffusion tensor model – which assumes anisotropic Gaussian diffusion – as a basis for all these comparisons. This model accommodates neither more complex directional dependencies nor deviations from the single-exponential decay, e.g. due to the presence of compartments with different diffusion constants or to restricted diffusion within the axons (Assaf and Cohen, 1998a, 1998b; Basser and Jones, 2002; Mulkern et al., 1999; Niendorf et al., 1996). In order to better account for non-mono-exponential (non-Gaussian) decay, diffusion kurtosis imaging (DKI) has been proposed (Jensen and Helpert, 2010; Jensen et al., 2005; Lu et al., 2006). This approach, particularly when using data collected along different axes to characterize the orientation dependence yields additional sensitivity towards tissue microstructure (Cheung et al., 2009; Hui et al., 2008) and confers several advantages. First, deviations from the Gaussian assumption, as expressed by the excess kurtosis along a given axis, are direct indicators of barriers along that particular axis. Second, DKI provides a more objective characterization of the diffusion propagator, in that the dependence of the estimated diffusivity on the b-value is eliminated or at least strongly reduced. However, the technique is certainly not without limitations. The most severe disadvantage is that the method requires that data be acquired over multiple b-values. For example, Cheung et al. (2009) used five non-zero b-values between 500 and 2500  $\text{s mm}^{-2}$  to estimate the direction dependent kurtosis in developing rats. Moreover, as is the case with diffusion tensor MRI, all that can be inferred from a change in the kurtosis – is that there is something in the tissue microstructure that is changing the way that molecules can diffuse. More kurtosis means more deviation from Gaussian diffusion propagator. Although one may interpret such changes as arising from a particular sub-component (e.g., “more kurtosis means more axonal membranes”) – such inferences are not substantiated. The kurtosis does not involve any biophysical model – and just arises from a mathematical expansion of the diffusion-weighted signal as a function of the b-value.

As mentioned earlier, an alternative way to account for the non-monoexponential nature of the b-value dependence of the signal has been proposed by Assaf et al. (2004). These authors proposed an approach, driven by a biophysical model, called the composite hindered and restricted model of diffusion (CHARMED), which assumes a combination of intra-axonal restricted and extra-axonal hindered

diffusion with different diffusivities. While additional b-values are needed, by varying the number of gradient directions with the b-value (such that more dense sampling of the angular space is performed as the b-value is increased), and using different sampling vectors for each b-value, Assaf and Basser (2005) could apply the CHARMED method using only 169 different diffusion weightings to human subjects, albeit only to an axial slab of 3 cm thickness with an isotropic resolution of 3 mm. The parameters of the CHARMED model, e.g., the volume fractions of the different compartments, hold great promise in delivering sensitive, informative and interpretable microstructural indices. De Santis et al. (in press) have recently shown how the quantities obtained from the CHARMED model can be used to infer the excess kurtosis, providing a link between these disparate analysis approaches.

As described above, a number of HARDI techniques have been developed to account for multiple fiber directions in a voxel. Scalar measures were developed to describe important properties of these ODFs. For example, Tuch (2004) proposed a number of such measures based on q-ball imaging. The generalized fractional anisotropy (GFA) is defined, in analogy to the FA, as the ratio of the standard deviation of the orientation densities in the different gradient directions to its root mean square. Hence, this measure somehow describes the “degree of variation” of the ODF. Also higher order moments are possible, such as generalized skewness and kurtosis (Cook et al., 2007). However, as the densities are not Gaussian distributed, this description is necessarily incomplete and can be misleading. Moreover, quantitative indices derived from higher order models than the tensor (such as the GFA) have not found widespread usage, and these measures remain “angular” measures because the radial part of the diffusion signal is never or rarely used/included.

## Interpretation

The interpretation of DW-MRI data is essentially a model based procedure, even if no formal, mathematically described model is invoked, i.e., the measured data are combined with a number of assumptions about the underlying processes and structures. These model assumptions always represent a simplification of reality, i.e., they neglect certain aspects of the true generative mechanism of the data. For the choice of the model, three aspects are important: (a) the quality and quantity of the available data; (b) which aspects of the underlying processes and structure one is interested in, i.e., which type of conclusion is to be drawn from the result; and (c) whether the model is adequate, i.e., to what extent the estimation of the parameters of interest is biased by the inevitable model simplifications. In the following we will briefly discuss these aspects.

A ubiquitous danger with any model-based approach is over-fitting, i.e., trying to extract more information from the data than they contain. A common example is the occurrence of spurious peaks in spherical deconvolution results. The phenomenon of overfitting triggers two immediate questions: (1) how to avoid it and (2) how to recognize it. The first question can be addressed comparatively easily, by ensuring adequate quantity (numbers of directions and b-values, voxel resolution) and quality (SNR) of data, and, if necessary by reducing the model complexity and by regularization (which also reduces the model complexity). The second question is a tricky one. If overfitting occurs, features in the solution start to depend mainly on noise. As noise is random, repetition of the experiment might reveal overfitting, as the noise dependent features in the solution will then turn out as unstable. In other words, here we would test the generalizability of the model. Often, anatomical knowledge might help to recognize overfitting. Here, some “gut-feeling” comes into play: if some unusual details occur in the results, one has to be suspicious and closely observe whether these features remain stable over several subjects of different experiments in the same subject.

While we favor refined models driven by the underlying biophysics as a way forward, we note that having such a model does not imply that the parameters can be interpreted unambiguously. They must still be interpreted with care. For example, complex models can have very correlated parameters, and unmodeled features in the data can lead to biases in some of the parameter estimates.

When selecting a particular analysis method, it should be borne in mind what type of conclusion will be drawn from the result. Very commonly one wants to infer on the local fiber directions or, more globally, on the course of fiber trajectories. For this type of conclusion, local models should be used that reflect the true angular structure of the diffusion propagator (almost invariably requiring something more than a single tensor model). In order to gain insight into the reproducibility or “determinedness” (precision) of the trajectories, some sort of probabilistic tracking scheme is recommended. In other cases, however, the question is simply whether orientation-dependent aspects of the microstructure have changed due to, e.g. illness, treatment, learning, etc., or are different between groups. Here, also the diffusion tensor, or derived quantities, such as the fractional anisotropy (FA), can be extremely useful, especially if the data quality (constrained perhaps by the time available for data acquisition) renders the use of more complex models risky. The danger lies in the interpretation. A difference in FA simply means that some orientation dependent aspects of the microstructure of the tissue are different. Any further interpretations, such as on the degree of myelination, axon density or indeed ‘integrity’ must be backed by strong theoretical foundations or additional data from other sources. Hence the appropriateness of a method depends on the type and quality of the data as well as on the purpose of the investigation.

## Conclusions

As we stated at the outset, the only thing that that we can say with any certainty in diffusion MRI is that we measure a signal change when a motion-sensitizing gradient is applied along a given axis. Inferring anything else is dependent on the quality of the model and the quality of the data. There are many mechanisms by which the diffusion weighted signal can be modulated. This includes but is not limited to, the myelination, the axon density, the axon diameter, the permeability of the membrane – but also, and importantly, the way in which the axons are laid out within the voxel. Thus one can have myelination, axon density and membrane permeability that is completely within normal range – but yet, if there is a difference in the architectural paradigm (*i.e.*, the manner in which the axons are laid out in the voxel), then there can be a difference in the anisotropy. The study of such differences in the architecture within the voxel could yield new insights into, for example, developmental trajectories or genetic influences.

However, as we have discussed in some depth, the ability to unambiguously map the layout of axons within a voxel by simply ‘listening’ to the outside of the voxel is a serious challenge. But – what should be absolutely clear is that using simplistic models for diffusion (such as the unimodal Gaussian tensor) will not provide those insights – and, moreover, the notion that one is looking at ‘white matter integrity’ should be abandoned. We are not suggesting that DT-MRI is redundant. Indeed, due to the fact that it measures the displacement of water molecules at the scale of tens of microns, it is *exquisitely* sensitive to any change in tissue microstructure – and therefore could provide a useful ‘first port of call’ in investigations of white matter in health, development and disease. However, one will quickly hit a brick-wall in interpretation if just the tensor model is used.

In the same way that scalar measures of anisotropy can be modulated by geometrical factors, the success of reconstructing a continuous path through the diffusion MR data field can be influenced by many factors including stochastic errors (Johnson RF and physiological noise) and deterministic errors. Again, differences in a tracking result might be found between two groups of subjects (*e.g.* controls *versus* patients) or a

tracking score found to correlate with performance on a task in a group of individuals, and this forms the basis for further investigation. However, asserting categorically that the change in those scores is being driven by a specific biological or physiological process is extremely problematic. Again, the only thing that can be inferred is that there is a difference in our ability to form a continuous path through the data field – which, in turn, is produced from a series of measurements of signal loss – all else is modeling assumption.

We hope that this article will help to clarify certain misconceptions that appear to be prevalent in the literature and provide good reasons for discontinuing the use of certain interpretative terminologies. We understand the motivation for introducing terms into the literature that allude to biological/physiological processes, as it is these terms that help to ‘sell’ a paper to the reader. However, we believe that just because we have a huge number of papers that report on the application of diffusion MRI using such inappropriate terms and interpretations, does not mean that the practice should continue. We therefore urge journal Editors and reviewers of manuscripts to challenge authors, who present interpretations such as ‘fiber count’, ‘white matter integrity’ and ‘connection strength’, to justify their usage of such terms – and if insufficient justification can be provided, to insist that they be removed from the manuscript. In summary, we present our list of recommendations.

## The do's

- a. Carefully consider the question(s) to be asked of the data and consider whether the data acquisition/analysis allows you to answer these questions.

As most of the recommendations given below (small voxels, many directions, high diffusion weighting, high SNR) are in mutual competition, the user has to decide where to invest the precious acquisition time. For simple questions such as unspecific white matter differences between two groups, there are minimal demands on the data acquisition and analysis, the diffusion tensor might suffice. On the other hand, a high SNR might be valuable to increase statistical power.

In contrast, detailed interpretations of differences in tissue microstructure demand far more sophisticated acquisition/analyses: higher or even multiple b-values as well as many directions are essential.

Likewise, tractography sufficient angular resolution and, even more importantly, high spatial resolution (voxel size), in conjunction with sophisticated local models, are absolutely crucial.

- b. Carefully consider the impact of pre-processing steps on the quantitative metrics to be derived from the diffusion-weighted signal. There is a multitude of software packages available to analyze diffusion-weighted MR data. We caution the reader that not all software packages pre-process the data in the same way – and this can lead to differences in data quality, potentially power to detect group differences/individual differences/correlations between DW-MRI-derived metrics and other measures (*e.g.* cognitive performance, disability *etc.*). Our sub-set of recommendations is as follows:

- For diffusion tensor estimation, choose a software package that provides non-linear estimation of the tensor without logarithmic transformation of the signal. If this is unavailable, then choose a routine that provides a *weighted* linear least squares fit to the log-transformed data. Many software packages in use simply use an ordinary linear least squares fit to the data, which ignores the heteroscedasticity introduced by the logarithmic transformation of the data. If available, we recommend to use robust estimation routines (Geman–McClure estimator, RESTORE), to reduce the impact of outliers on the data and to avoid transients in the data impacting on conclusions.
- We also recommend the deployment of methods to ameliorate CSF-based partial volume artefacts. If use of a FLAIR-based

diffusion-weighted MR acquisition is appropriate, then this could be utilized. Otherwise, modeling approaches that account for CSF-based contamination (e.g., by fitting two compartments to the signal – with one assigned to tissue, and one assigned to CSF), should be used. We do not recommend using any local or global estimate of tissue volume to estimate CSF-contamination.

- When correcting for eddy-currents, we recommend choosing a software package/routine that will modulate the signal by the determinant of the Jacobian transformation matrix. This simple step is overlooked in many software packages.
  - Likewise, when correcting for subject motion, ensure that any rotations that are applied to a given diffusion-weighted volume, are also applied to the encoding vectors. Again, this is a trivial step – but is not included in many pre-processing pipelines.
  - Always inspect the raw data prior to modeling, and after fitting the model. Examining the residuals is extremely useful in identifying systematic errors in the data and to identify inadequacies in the model.
- c. For reconstruction of the orientation density function, use the highest sensitivity DWI sequence available.  
Higher diffusion-weightings provide higher angular resolution when resolving complex fiber architectures. However, see next point....
- d. Whatever maximum diffusion-weighting is appropriate for the question being asked, ensure that the SNR in the images never drops below 3:1.  
When dealing with magnitude data, the noise-distribution is non-Gaussian, which biases measurements at low SNRs – unless appropriate noise models (Rician/non-central chi) are used. We stress this is a bare minimum. DO check to see that the SNR used is fit for purpose, especially with regard to the end application.
- e. Use High Angular Resolution Diffusion Imaging (HARDI) whenever possible, using the largest number of gradient orientations that scanner and subject time allows.  
While this is of clear benefit for resolving multiple fiber orientations, it is also important to ensure statistical rotational invariance of simple metrics such as FA and mean diffusivity derived from the tensor model.
- f. Use the smallest isotropic voxels possible, consistent with this limiting SNR.  
The higher the resolution, the better chance of reconstructing finer pathways – and, moreover, the less ‘powder-averaging’ of different fiber orientations within the voxel.
- g. For tractography, use software that accounts for fiber crossings.  
With the number of voxels containing 2 or more fiber populations in the brain estimated to be in the region of 90%, it is clear that failing to account for crossing fiber configurations will lead to erroneous fiber trajectory reconstructions.

### The don'ts

- a. Don't assume that the principal eigenvector of a diffusion tensor is a good indication of the actual fiber orientations in all voxels. Although in a limited set of places (where the bundle-to-voxel size is favorable and all fibers are highly parallel in the voxel), the principal eigenvector may do a good job, it is unsafe to use this simple model throughout the whole brain.
- b. Don't assume that tractography using a single diffusion tensor will be adequate for all fiber trajectories in the brain. Most fibers cross with others, diverge/converge, twist or kink at some point – and so single tensor-based tracking will result in fiber pathways that are always in error somewhere along their length.
- c. Except in the case of clinically-diagnosed conditions explicitly impacting on white matter, including demyelinating disease, chronic

ischemia and tumor infiltration, don't use the term ‘white matter integrity’.

Use of the term ‘white matter integrity’ is especially discouraged when talking about individual differences in white matter in healthy individuals.

- d. Don't confuse fractional anisotropy with ‘white matter integrity’.  
FA is naturally low in normal white matter areas where fibers cross.
- e. Don't use the phrase ‘fiber count’ when referring to data derived from diffusion MRI.  
There are multiple reasons why the number of fibers reconstructed between two regions may be different – some related to real anatomy, others related to performance of the tracking algorithm. ‘Streamline count’ is a far preferable term.
- f. Don't use tractography to provide a quantitative estimate of ‘connection strength’.  
Tractography algorithms largely deploy the orientation information encoded in the DW-MRI signal. To date, no index derived from tractography has been proposed to quantify ‘connection strength’ in a physiological or anatomical context. It is not possible to reliably estimate the number of axonal projections, for example, from tractography.  
Our final quote, in keeping with the title of this manuscript, is “Do continue to use diffusion MRI – it is a fantastic technique for understanding the brain – but don't over-interpret, mis-interpret and misuse the terminology!”

### References

- Acosta-Cabrero, J., Williams, G.B., Pengas, G., Nestor, P.J., 2010. Absolute diffusivities define the landscape of white matter degeneration in Alzheimer's disease. *Brain* 133, 529–539.
- Aganj, I., Lenglet, C., Sapiro, E., Yacoub, E., Ugurbil, K., et al., 2010. Reconstruction of the orientation distribution function in single and multiple shell q-ball imaging with constant solid angle. *Magn. Reson. Med.* 64, 554–566.
- Aja-Fernández, S., Niethammer, M., Kubicki, M., Shenton, M.E., Westin, C.-F., 2008. Restoration of DWI data using a Rician LMMSE estimator. *IEEE Trans. Med. Imaging* 27, 1389–1403.
- Alexander, D.C., 2005a. Maximum entropy spherical deconvolution for diffusion MRI. In: Christensen, G.E., Soga, M. (Eds.), *Information Processing in Medical Imaging, Proceedings*, pp. 76–87.
- Alexander, D., 2005b. Multiple-fiber reconstruction algorithms for diffusion MRI. *Ann. N. Y. Acad. Sci.* 1064, 113–133.
- Alexander, D.C., Barker, G.J., Arridge, S.R., 2002. Detection and modeling of non-Gaussian apparent diffusion coefficient profiles in human brain data. *Magn. Reson. Med.* 48, 331–340.
- Alexander, D., Hubbard, P., Hall, M., Moore, E., Ptito, M., et al., 2010. Orientationally invariant indices of axon diameter and density from diffusion MRI. *NeuroImage* 52, 1374–1389.
- Anderson, A.W., Gore, J.C., 1994. Analysis and correction of motion artifacts in diffusion weighted imaging. *Magn. Reson. Med.* 32, 379–387.
- Assaf, Y., Basser, P., 2005. Composite hindered and restricted model of diffusion (charmed) MR imaging of the human brain. *NeuroImage* 27, 48–58.
- Assaf, Y., Cohen, Y., 1998a. *In vivo* and *in vitro* bi-exponential diffusion of N-acetyl aspartate (NAA) in rat brain: a potential structural probe? *NMR Biomed.* 11, 67–74.
- Assaf, Y., Cohen, Y., 1998b. Non-mono-exponential attenuation of water and N-acetyl aspartate signals due to diffusion in brain tissue. *J. Magn. Reson.* 131, 69–85.
- Assaf, Y., Cohen, Y., 2000. Assignment of the water slow-diffusing component in the central nervous system using q-space diffusion MRS: implications for fiber tract imaging. *Magn. Reson. Med.* 43, 191–199.
- Assaf, Y., Freidlin, R., Rohde, G., Basser, P., 2004. New modeling and experimental framework to characterize hindered and restricted water diffusion in brain white matter. *Magn. Reson. Med.* 52, 965–978.
- Assaf, Y., Blumenfeld-Katzir, T., Yovel, Y., Basser, P.J., 2008. AxCaliber: a method for measuring axon diameter distribution from diffusion MRI. *Magn. Reson. Med.* 59, 1347–1354.
- Avants, B.B., Cook, P.A., Ungar, L., Gee, J.C., Grossman, M., 2010. Dementia induces correlated reductions in white matter integrity and cortical thickness: a multivariate neuroimaging study with sparse canonical correlation analysis. *NeuroImage* 50, 1004–1016.
- Bammer, R., Stollberger, R., Augustin, M., Simbrunner, J., Offenbacher, H., et al., 1999. Diffusion-weighted imaging with navigated interleaved echo-planar imaging and a conventional gradient system. *Radiology* 211, 799–806.
- Basser, P.J., 1995. Inferring microstructural features and the physiological state of tissues from diffusion-weighted images. *NMR Biomed.* 8, 333–344.
- Basser, P.J., Jones, D.K., 2002. Diffusion-tensor MRI: theory, experimental design and data analysis – a technical review. *NMR Biomed.* 15, 456–467.

- Basser, P., Mattiello, J., Le Bihan, D., 1994a. MR diffusion tensor spectroscopy and imaging. *Biophys. J.* 66, 259–267.
- Basser, P.J., Mattiello, J., LeBihan, D., 1994b. Estimation of the effective self-diffusion tensor from the NMR spin echo. *J. Magn. Reson. B* 103, 247–254.
- Beaulieu, C., 2002. The basis of anisotropic water diffusion in the nervous system – a technical review. *NMR Biomed.* 15, 435–455.
- Behrens, T., Johansen-Berg, H. (Eds.), 2009. *Diffusion MRI: from quantitative measurement to in-vivo neuroanatomy*. Elsevier.
- Behrens, T.E., Woolrich, M.W., Jenkinson, M., Johansen-Berg, H., Nunes, R.G., et al., 2003. Characterization and propagation of uncertainty in diffusion-weighted MR imaging. *Magn. Reson. Med.* 50, 1077–1088.
- Behrens, T.E.J., Berg, H.J., Jbabdi, S., Rushworth, M.F.S., Woolrich, M.W., 2007. Probabilistic diffusion tractography with multiple fibre orientations: what can we gain? *NeuroImage* 34, 144–155.
- Bodini, B., Khaleeli, Z., Cercignani, M., Miller, D.H., Thompson, A.J., et al., 2009. Exploring the relationship between white matter and gray matter damage in early primary progressive multiple sclerosis: an *in vivo* study with TBSS and VBM. *Hum. Brain Mapp.* 30, 2852–2861.
- Breuer, F.A., Blaimer, M., Heidemann, R.M., Mueller, M.F., Griswold, M.A., Jakob, P.M., 2005. Controlled aliasing in parallel imaging results in higher acceleration (CAIPI-RINHA) for multi-slice imaging. *Magn. Reson. Med.* 53, 684–691.
- Brion, V., Poupon, C., Riff, O., Aja-Fernández, S., Tristán-Vega, A., et al., 2011. Parallel MRI noise correction: an extension of the LMMSE to non central chi distributions. *Med. Image Comput. Comput. Assist. Interv.* 14.
- Butts, K., deCrespigny, A., Pauly, J.M., Moseley, M., 1996. Diffusion-weighted interleaved echo-planar imaging with a pair of orthogonal navigator echoes. *Magn. Reson. Med.* 35, 763–770.
- Butts, K., Pauly, J., deCrespigny, A., Moseley, M., 1997. Isotropic diffusion-weighted and spiral-navigated interleaved EPI for routine imaging of acute stroke. *Magn. Reson. Med.* 38, 741–749.
- Callaghan, P.T., Eccles, C.D., Xia, Y., 1988. NMR microscopy of dynamic displacements – k-spaced and q-space imaging. *J. Phys. E: Sci. Instrum.* 21, 820–822.
- Callaghan, P.T., Coy, A., Macgowan, D., Packer, K.J., Zelaya, F.O., 1991. Diffraction-like effects in NMR diffusion studies of fluids in porous solids. *Nature* 351, 467–469.
- Cercignani, M., 2010. Strategies for patient-control comparison of diffusion MR data. In: Jones, D.K. (Ed.), *Diffusion MRI: Theory, Methods and Applications*. Oxford University Press.
- Cercignani, M., Alexander, D., 2006. Optimal acquisition schemes for *in vivo* quantitative magnetization transfer MRI. *Magn. Reson. Med.* 56, 803–810.
- Chang, L.C., Jones, D.K., Pierpaoli, C., 2005. RESTORE: robust estimation of tensors by outlier rejection. *Magn. Reson. Med.* 53, 1088–1095.
- Chang, L., Walker, L., Pierpaoli, C., 2012. Informed RESTORE: a method for robust estimation of diffusion tensor from low redundancy datasets in the presence of physiological noise artifacts. *Magn. Reson. Med.* (pub ahead of print). <http://dx.doi.org/10.1002/mrm.24173>.
- Chen, Y., An, H., Zhu, H., Stone, T., Smith, J.K., et al., 2009. White matter abnormalities revealed by diffusion tensor imaging in non-demented and demented HIV+ patients. *NeuroImage* 47, 1154–1162.
- Cheng, Y., Chou, K.-H., Chen, I.Y., Fan, Y.-T., Decety, J., et al., 2010. Atypical development of white matter microstructure in adolescents with autism spectrum disorders. *NeuroImage* 50, 873–882.
- Cheung, M.M., Hui, E.S., Chan, K.C., Helpner, J.A., Qi, L., et al., 2009. Does diffusion kurtosis imaging lead to better neural tissue characterization? A rodent brain maturation study. *NeuroImage* 45, 386–392.
- Chou, M.C., Lin, Y.R., Huang, T.Y., Wang, C.Y., Chung, H.W., et al., 2005. FLAIR diffusion-tensor MR tractography: comparison of fiber tracking with conventional imaging. *Am. J. Neuroradiol.* 26, 591–597.
- Chung, S.W., Lu, Y., Henry, R.G., 2006. Comparison of bootstrap approaches for estimation of uncertainties of DTI parameters. *NeuroImage* 33, 531–541.
- Ciccarelli, O., Behrens, T.E., Johansen-Berg, H., Talbot, K., Orrell, R.W., et al., 2009. Investigation of white matter pathology in ALS and PLS using tract-based spatial statistics. *Hum. Brain Mapp.* 30, 615–624.
- Clark, C.A., Le Bihan, D., 2000. Water diffusion compartmentation and anisotropy at high b values in the human brain. *Magn. Reson. Med.* 44, 852–859.
- Clark, C.A., Hedehus, M., Moseley, M.E., 2002. *In vivo* mapping of the fast and slow diffusion tensors in human brain. *Magn. Reson. Med.* 47, 623–628.
- Clarke, R.A., Scifo, P., Rizzo, G., Dell'Acqua, F., Scotti, G., et al., 2008. Noise correction on Rician distributed data for fibre orientation estimators. *IEEE Trans. Med. Imaging* 27, 1242–1251.
- Cohen, Y., Assaf, Y., 2002. High b-value q-space analyzed diffusion-weighted MRS and MRI in neuronal tissues – a technical review. *NMR Biomed.* 15, 516–542.
- Concha, L., Gross, D.W., Beaulieu, C., 2005. Diffusion tensor tractography of the limbic system. *Am. J. Neuroradiol.* 26, 2267–2274.
- Conturo, T.E., Lori, N.F., Cull, T.S., Akbudak, E., Snyder, A.Z., et al., 1999. Tracking neuronal fiber pathways in the living human brain. *Proc. Natl. Acad. Sci. U. S. A.* 96, 10422–10427.
- Cook, P., Symms, M., Boulby, P., Alexander, D., 2007. Optimal acquisition orders of diffusion-weighted MRI measurements. *J. Magn. Reson. Imaging* 25, 1051–1058.
- Cory, D.G., Garroway, A.N., 1990. Measurement of translational displacement probabilities by NMR – an indicator of compartmentation. *Magn. Reson. Med.* 14, 435–444.
- Cykowski, M.D., Fox, P.T., Ingham, R.J., Ingham, J.C., Robin, D.A., 2010. A study of the reproducibility and etiology of diffusion anisotropy differences in developmental stuttering: a potential role for impaired myelination. *NeuroImage* 52, 1495–1504.
- Damoiseaux, J.S., Smith, S.M., Witter, M.R., Sanz-Arigita, E.J., Barkhof, F., et al., 2009. White matter tract integrity in aging and Alzheimer's disease. *Hum. Brain Mapp.* 30, 1051–1059.
- Davis, S.W., Dennis, N.A., Buchler, N.G., White, L.E., Madden, D.J., et al., 2009. Assessing the effects of age on long white matter tracts using diffusion tensor tractography. *NeuroImage* 46, 530–541.
- De Santis, S., Assaf, Y., Jones, D., 2012. Using the biophysical CHARMED model to elucidate the underpinnings of contrast in diffusional kurtosis analysis of diffusion-weighted MRI. *Magn. Reson. Mater. Phys. Biol. Med.* 25 (4), 267–276.
- Dell'Acqua, F., Scifo, P., Rizzo, G., Catani, M., Simmons, A., et al., 2010. A modified damped Richardson–Lucy algorithm to reduce isotropic background effects in spherical deconvolution. *NeuroImage* 49, 1446–1458.
- Dell'Acqua, F., Simmons, A., Williams, S., Catani, M., 2012. Can spherical deconvolution provide more information than fiber orientations? Hindrance modulated orientational anisotropy, a true-tract specific index to characterize white matter diffusion. *Hum. Brain Mapp.* (pub ahead of print). <http://dx.doi.org/10.1002/mrm.24173>.
- Deoni, S.C.L., Rutt, B.K., Pierpaoli, C., Jones, D.K., 2008. Gleaning multi-component T<sub>1</sub> and T<sub>2</sub> information from steady-state imaging data. *Magnetic Resonance in Medicine* 60, 1372–1387.
- Descoteaux, M., 2008. High Angular Resolution Diffusion MRI: from local estimation to segmentation and tractography: Université de Nice – Sophia Antipolis.
- Descoteaux, M., Angelino, E., Fitzgibbons, S., Deriche, R., 2006. Apparent diffusion coefficients from high angular resolution diffusion imaging: estimation and applications. *Magn. Reson. Med.* 56, 395–410.
- Descoteaux, M., Angelino, E., Fitzgibbons, S., Deriche, R., 2007. Regularized, fast, and robust analytical Q-ball imaging. *Magn. Reson. Med.* 58, 497–510.
- Descoteaux, M., Deriche, R., Knösche, T.R., Anwander, A., 2009. Deterministic and probabilistic tractography based on complex fibre orientation distributions. *IEEE Trans. Med. Imaging* 28, 269–286.
- Dietrich, O., Raya, J.G., Reeder, S.B., Ingrisch, M., Reiser, M.F., et al., 2008. Influence of multichannel combination, parallel imaging and other reconstruction techniques on MRI noise characteristics. *Magn. Reson. Imaging* 26, 754–762.
- Doneva, M., Boerner, P., Eggers, H., Stehning, C., Senegas, J., et al., 2010. Compressed sensing reconstruction for magnetic resonance parameter mapping. *Magn. Reson. Med.* 64, 1114–1120.
- Donoho, D.L., 2006. Compressed Sensing. *IEEE Transactions on Information Theory* 52 (4), 1289–1306.
- Faria, A.V., Zhang, J., Oishi, K., Li, X., Jiang, H., et al., 2010. Atlas-based analysis of neurodevelopment from infancy to adulthood using diffusion tensor imaging and applications for automated abnormality detection. *NeuroImage* 52, 415–428.
- Feinberg, D.A., Moeller, S., Smith, S.M., Auerbach, E., Ramanna, S., et al., 2010. Multiplexed echo planar imaging for sub-second whole brain fMRI and fast diffusion imaging. *PLoS One* 5.
- Fletcher, P.T., Whitaker, R.T., Tao, R., DuBray, M.B., Froehlich, A., et al., 2010. Microstructural connectivity of the arcuate fasciculus in adolescents with high-functioning autism. *NeuroImage* 51, 1117–1125.
- Flöel, A., de Vries, M.H., Scholz, J., Breitenstein, C., Johansen-Berg, H., 2009. White matter integrity in the vicinity of Broca's area predicts grammar learning success. *NeuroImage* 47, 1974–1981.
- Freidlin, R., Özarslan, E., Komlosh, M., Chang, L., Koay, C., et al., 2007. Parsimonious model selection for tissue segmentation and classification applications: a study using simulated and experimental DTI data. *IEEE Trans. Med. Imaging* 26, 1576–1584.
- Gold, B.T., Powell, D.K., Andersen, A.H., Smith, C.D., 2010. Alterations in multiple measures of white matter integrity in normal women at high risk for Alzheimer's disease. *NeuroImage* 52, 1487–1494.
- Goodlett, C.B., Fletcher, P.T., Gilmore, J.H., Gerig, G., 2009. Group analysis of DTI fiber tract statistics with application to neurodevelopment. *NeuroImage* 45, S133–S142.
- Grinberg, F., Farrher, E., Kaffanke, J., Oros-Peusquens, A.-M., Shah, N.J., 2011. Non-Gaussian diffusion in human brain tissue at high b-factors as examined by a combined diffusion kurtosis and biexponential diffusion tensor analysis. *NeuroImage* 57, 1087–1102.
- Griswold, M., Jakob, P., Heidemann, R., Nittka, M., Jellus, V., et al., 2002. Generalized autocalibrating partially parallel acquisitions (GRAPPA). *Magn. Reson. Med.* 47, 1202–1210.
- Gudbjartsson, H., Patz, S., 1995. The Rician distribution of noisy MRI data. *Magn. Reson. Med.* 34, 910–914.
- Hagmann, P., Kuran, M., Gigandet, X., Thiran, P., Wedeen, V.J., et al., 2007. Mapping human whole-brain structural networks with diffusion MRI. *PLoS One* 2, e597.
- Hagmann, P., Cammoun, L., Gigandet, X., Meuli, R., Honey, C.J., et al., 2008. Mapping the structural core of human cerebral cortex. *PLoS Biol.* 6, e159.
- Hagmann, P., Cammoun, L., Gigandet, X., Gerhard, S., Ellen Grant, P., et al., 2010. MR connectomics: principles and challenges. *J. Neurosci.* 30, 1494–1504.
- Haroon, H.A., Morris, D.M., Embleton, K.V., Alexander, D.C., Parker, G.J.M., 2009. Using the model-based residual bootstrap to quantify uncertainty in fiber orientations from Q-ball analysis. *IEEE Trans. Med. Imaging* 28, 535–550.
- Heidemann, R.M., Anwander, A., Feiwel, T., Knösche, T., Turner, R., et al., 2012. k-space and q-space: combining ultrahigh spatial and angular resolution in diffusion imaging using ZOOMPPA at 7T. *NeuroImage* 60 (2), 967–978.
- Henkelman, R.M., 1985. Measurement of signal intensities in the presence of noise in MR images. *Med. Phys.* 12, 232–233.
- Honey, C.J., Sporns, O., Cammoun, L., Gigandet, X., Thiran, J.P., et al., 2009. Predicting human resting-state functional connectivity from structural connectivity. *Proc. Natl. Acad. Sci. U. S. A.* 106, 2035–2040.
- Huang, H., Zhang, J., van Zijl, P., Mori, S., 2004. Analysis of noise effects on DTI-based tractography using the brute-force and multi-ROI approach. *Magn. Reson. Med.* 52, 559–565.
- Hui, E.S., Cheung, M.M., Qi, L., Wu, E.X., 2008. Towards better MR characterization of neural tissues using directional diffusion kurtosis analysis. *NeuroImage* 42, 122–134.

- Inglis, B.A., Bossart, E.L., Buckley, D.L., Wirth, E.D., Mareci, T.H., 2001. Visualization of neural tissue water compartments using biexponential diffusion tensor MRI. *Magn. Reson. Med.* 45, 580–587.
- Iwata, N.K., Kwan, J.Y., Danielian, L.E., Butman, J.A., Tovar-Moll, F., et al., 2011. White matter alterations differ in primary lateral sclerosis and amyotrophic lateral sclerosis. *Brain* 134, 2642–2655.
- Jahng, G.-H., Xu, S., Weiner, M.W., Meyerhoff, D.J., Park, S., et al., 2011. DTI studies in patients with Alzheimer's disease, mild cognitive impairment, or normal cognition with evaluation of the intrinsic background gradients. *Neuroradiology* 53, 749–762.
- Jansons, K.M., Alexander, D.C., 2003. Persistent angular structure: new insights from diffusion magnetic resonance imaging data. *Inverse Prob.* 19, 1031–1046.
- Jensen, J.H., Helpert, J.A., 2010. MRI quantification of non-Gaussian water diffusion by kurtosis analysis. *NMR Biomed.* 23, 698–710.
- Jensen, J.H., Helpert, J.A., Ramani, A., Lu, H.Z., Kaczynski, K., 2005. Diffusional kurtosis imaging: the quantification of non-Gaussian water diffusion by means of magnetic resonance imaging. *Magn. Reson. Med.* 53, 1432–1440.
- Jeurissen, B., Leemans, A., Tournier, J.-D., Jones, D., Sijbers, J. (in press) Investigating the prevalence of complex fiber configurations in white matter tissue with diffusion MRI. *Hum. Brain Mapp.*
- Jeurissen, B., Leemans, A., Tournier, J.-D., Jones, D., Sijbers, J., 2010. Estimating the 1759 Number of Fiber Orientations in Diffusion MRI Voxels: A Constrained Spherical Q141760 Deconvolution Study. *Proceedings of the International Society for Magnetic Resonance in Medicine, Stockholm, Sweden*. p. 573. <http://dx.doi.org/10.1002/hbm.22099>.
- Johansen-Berg, H., 2010. Behavioural relevance of variation in white matter microstructure. *Curr. Opin. Neurol.* 23, 351–358.
- Jones, D.K., 2003. Determining and visualizing uncertainty in estimates of fiber orientation from diffusion tensor MRI. *Magn. Reson. Med.* 49, 7–12.
- Jones, D.K., 2004. The effect of gradient sampling schemes on measures derived from diffusion tensor MRI: a Monte Carlo study. *Magn. Reson. Med.* 51, 807–815.
- Jones, D.K., 2008. Tractography gone wild: probabilistic fibre tracking using the wild bootstrap with diffusion tensor MRI. *IEEE Trans. Med. Imaging* 27, 1268–1274.
- Jones, D.K. (Ed.), 2010a. *Diffusion MRI: Theory, Methods and Applications*. Oxford University Press.
- Jones, D.K., 2010b. Challenges and limitations of quantifying connectivity in the human brain *in vivo* with diffusion MRI. *Imaging Med.* 2, 341–355.
- Jones, D.K., 2010c. Precision and accuracy in diffusion tensor MRI. *Top. Magn. Reson. Imaging Med.* 21, 87–99.
- Jones, D.K., Basser, P.J., 2004. "Squashing peanuts and smashing pumpkins": how noise distorts diffusion-weighted MR data. *Magn. Reson. Med.* 52, 979–993.
- Jones, D.K., Cercignani, M., 2010. Twenty-five pitfalls in the analysis of diffusion MRI data. *NMR Biomed.* 23, 803–820.
- Jones, D.K., Leemans, A., 2011. Diffusion tensor imaging. In: *Modo, M., Bulte, J.W.M. (Eds.), Magnetic Resonance Neuroimaging: Methods and Protocols Humana Press*, pp. 127–144.
- Jones, D.K., Pierpaoli, C., 2005a. Confidence mapping in diffusion tensor magnetic resonance imaging tractography using a bootstrap approach. *Magn. Reson. Med.* 53, 1143–1149.
- Jones, D.K., Pierpaoli, C., 2005b. The contribution of cardiac pulsation to variability in Q161787 tractography results. *Proceedings of the International Society for Magnetic Resonance in Medicine, Miami*, p. 225.
- Jones, D.K., Travis, A., Eden, G., Pierpaoli, C., Basser, P., 2005a. PASTA: pointwise assessment of streamline tractography attributes. *Magn. Reson. Med.* 53, 1462–1467.
- Jones, D.K., Catani, M., Pierpaoli, C., Reeves, S., Shergill, S., et al., 2005b. Age effects on diffusion tensor magnetic resonance imaging tractography measures of frontal cortex connections in schizophrenia. *Hum. Brain Mapp.* 27, 230–238.
- Jones, D.K., Catani, M., Pierpaoli, C., Reeves, S., Shergill, S., et al., 2005c. A diffusion tensor magnetic resonance imaging study of frontal cortex connections in very late-onset schizophrenia-like psychosis. *Am. J. Geriatr. Psychiatry* 13, 1092–1099.
- Kaden, E., Knösche, T.R., Anwander, A., 2007. Parametric spherical deconvolution: inferring anatomical connectivity using diffusion MR imaging. *NeuroImage* 37, 474–488.
- Kanai, R., Rees, G., 2011. The structural basis of inter-individual differences in human behaviour and cognition. *Nat. Rev. Neurosci.* 12, 231–242.
- Kärger, J., Pfeifer, H., Heink, W., 1988. Principles and application of self-diffusion measurements by nuclear magnetic resonance. *Adv. Magn. Reson.* 12, 1–89.
- Kiselev, V., 2010. The cumulant expansion: an overarching mathematical framework for understanding diffusion NMR. In: *Jones, D.K. (Ed.), Diffusion MRI: Theory, Methods and Applications*. Oxford University Press.
- Klingberg, T., Vaidya, C.J., Gabrieli, J.D.E., Moseley, M.E., Hedehus, M., 1999. Myelination and organization of the frontal white matter in children: a diffusion tensor MRI study. *Neuroreport* 10, 2817–2821.
- Koay, C.G., Chang, L.-C., Carew, J.D., Pierpaoli, C., Basser, P.J., 2006. A unifying theoretical and algorithmic framework for least squares methods of estimation in diffusion tensor imaging. *J. Magn. Reson.* 182, 115–125.
- Koay, C.G., Özarslan, E., Basser, P.J., 2009. A signal transformation framework for correcting the noise floor and its applications in MRI. *J. Magn. Reson.* 197, 108–119.
- Koch, M.A., Norris, D.G., Hund-Georgiadis, M., 2002. An investigation of functional and anatomical connectivity using magnetic resonance imaging. *NeuroImage* 16, 241–250.
- Kochunov, P., Ramage, A.E., Lancaster, J.L., Robin, D.A., Narayana, S., et al., 2009. Loss of cerebral white matter structural integrity tracks the gray matter metabolic decline in normal aging. *NeuroImage* 45, 17–28.
- Kolind, S., Deoni, S., 2010. Rapid three-dimensional multicomponent relaxation imaging of the cervical spinal cord. *Magn. Reson. Med.* 65, 551–556.
- Kristoffersen, A., 2009. Diffusion measurements and diffusion tensor imaging with noisy magnitude data. *J. Magn. Reson. Imaging* 29, 237–241.
- Landman, B.A., Wan, H., Bogovic, J.A., Bazin, P.-L., Prince, J.L., 2010. Resolution of crossing fibers with constrained compressed sensing using traditional diffusion tensor MRI. In: *Dawant, B., Haynor, D. (Eds.), Medical Imaging 2010: Image Processing*.
- Landman, B., Bogovic, J., Wan, H., Elshahab, Y.F., Bazin, P., et al., 2012. Resolution of crossing fibers with constrained compressed sensing using diffusion tensor MRI. *NeuroImage* 59 (3), 2175–2186.
- Larkman, D.J., Hajnal, J.V., Herlihy, A.H., Coutts, G.A., Young, I.R., Ehnholm, G., 2001. Use of multicoil arrays for separation of signal from multiple slices simultaneously excited. *J. Magn. Reson. Imaging* 13, 313–317.
- Lazar, M., Alexander, A., 2003. An error analysis of white matter tractography methods: synthetic diffusion tensor field simulations. *NeuroImage* 20, 1140–1153.
- Le Bihan, D., 2007. The 'wet mind': water and functional neuroimaging. *Phys. Med. Biol.* 52, R57–R90.
- Le Bihan, D., Breton, E., 1985. *In vivo* magnetic resonance imaging of diffusion I. *C. R. Acad. Sci. II* 301, 1109–1112.
- Le Bihan, D., Breton, E., Lallemand, D., Grenier, P., Cabanis, E., et al., 1986. Magnetic resonance imaging of intravoxel incoherent motions – application to diffusion and perfusion in neurologic disorders. *Radiology* 161, 401–407.
- Le Bihan, D., Poupon, C., Amadon, A., Lethimonnier, F., 2006. Artifacts and pitfalls in diffusion MRI. *J. Magn. Reson. Imaging* 24, 478–488.
- Lebel, C., Caverhill-Godkewitsch, S., Beaulieu, C., 2010. Age-related regional variations of the corpus callosum identified by diffusion tensor tractography. *NeuroImage* 52, 20–31.
- Lee, B., Park, J.-Y., Jung, W.H., Kim, H.S., Oh, J.S., et al., 2010. White matter neuroplastic changes in long-term trained players of the game of "Baduk" (GO): a voxel-based diffusion-tensor imaging study. *NeuroImage* 52, 9–19.
- Leemans, A., Jones, D.K., 2009. The B-matrix must be rotated when correcting for subject motion in DTI data. *Magn. Reson. Med.* 61, 1336–1349.
- Liu, C.L., Bammer, R., Moseley, M.E., 2003. Generalized diffusion tensor imaging (GDTI): a method for characterizing and imaging diffusion anisotropy caused by non-Gaussian diffusion. *Isr. J. Chem.* 43, 145–154.
- Liu, C., Bammer, R., Acar, B., Moseley, M., 2004. Characterizing non-Gaussian diffusion by using generalized diffusion tensors. *Magn. Reson. Med.* 51, 924–937.
- Liu, B., Li, J., Yu, C., Li, Y., Liu, Y., et al., 2010. Haplotypes of catechol-O-methyltransferase modulate intelligence-related brain white matter integrity. *NeuroImage* 50, 243–249.
- Lori, N., Akbudak, E., Shimony, J., Cull, T., Snyder, A., et al., 2002. Diffusion tensor fiber tracking of human brain connectivity: acquisition methods, reliability analysis and biological results. *NMR Biomed.* 15, 494–515.
- Lu, H.Z., Jensen, J.H., Ramani, A., Helpert, J.A., 2006. Three-dimensional characterization of non-Gaussian water diffusion in humans using diffusion kurtosis imaging. *NMR Biomed.* 19, 236–247.
- Lustig, M., Lustig, Donoho, D., Donoho, Pauly, J.M., 2007. Sparse MRI: The application of compressed sensing for rapid MR imaging. *Magnetic Resonance in Medicine* 58, pp. 1182–1195.
- Maier, S.E., Mulkern, R.V., 2008. Biexponential analysis of diffusion-related signal decay in normal human cortical and deep gray matter. *Magn. Reson. Imaging* 26, 897–904.
- Maier, S.E., Vajapeyam, S., Mamata, H., Westin, C.F., Jolesz, F.A., et al., 2004. Biexponential diffusion tensor analysis of human brain diffusion data. *Magn. Reson. Med.* 51, 321–330.
- Menke, R.A., Scholz, J., Miller, K.L., Deoni, S., Jbabdi, S., et al., 2009. MRI characteristics of the substantia nigra in Parkinson's disease: a combined quantitative T1 and DTI study. *NeuroImage* 47, 435–441.
- Menzel, M.I., Tan, E.T., Khare, K., Sperl, J.J., King, K.F., et al., 2011. Accelerated diffusion spectrum imaging in the human brain using compressed sensing. *Magn. Reson. Med.* 66, 1226–1233.
- Metzler-Baddeley, C., O'Sullivan, M.J., Bells, S., Pasternak, O., Jones, D.K., 2012. How and how not to correct for CSF-contamination in diffusion MRI. *NeuroImage* 59, 1394–1403.
- Michailovich, O., Rathi, Y., 2010. Fast and accurate reconstruction of HARDI data using compressed sensing. In: *Jiang, T., Navab, B., Pluim, J.P.W., Viergever, M.A. (Eds.), Medical Image Computing and Computer-Assisted Intervention - Miccai 2010*, pp. 607–614. Pt 1.
- Michailovich, O., Rathi, Y., Dolui, S., 2011. Spatially regularized compressed sensing for high angular resolution diffusion imaging. *IEEE Trans. Med. Imaging* 30, 1100–1115.
- Michielse, S., Coupland, N., Camicioli, R., Carter, R., Seres, P., et al., 2010. Selective effects of aging on brain white matter microstructure: a diffusion tensor imaging tractography study. *NeuroImage* 52, 1190–1201.
- Mielke, M.M., Kozauer, N.A., Chan, K.C.G., George, M., Toroney, J., et al., 2009. Regionally-specific diffusion tensor imaging in mild cognitive impairment and Alzheimer's disease. *NeuroImage* 46, 47–55.
- Mori, S., van Zijl, P.C., 2002. Fiber tracking: principles and strategies – a technical review. *NMR Biomed.* 15, 468–480.
- Mori, S., Crain, B.J., Chacko, V.P., van Zijl, P.C.M., 1999. Three-dimensional tracking of axonal projections in the brain by magnetic resonance imaging. *Ann. Neurol.* 45, 265–269.
- Moseley, M., 2002. Diffusion tensor imaging and aging – a review. *NMR Biomed.* 15, 553–560.
- Mulkern, R.V., Gudbjartsson, H., Westin, C.F., Zengingonul, H.P., Gartner, W., et al., 1999. Multi-component apparent diffusion coefficients in human brain. *NMR Biomed.* 12, 51–62.
- Mulkern, R.V., Vajapeyam, S., Robertson, R.L., Caruso, P.A., Rivkin, M.J., et al., 2001. Biexponential apparent diffusion coefficient parametrization in adult vs newborn brain. *Magn. Reson. Imaging* 19, 659–668.

- Neuner, I., Kupriyanova, Y., Stöcker, T., Huang, R., Posnansky, O., et al., 2010. White-matter abnormalities in Tourette syndrome extend beyond motor pathways. *NeuroImage* 51, 1184–1193.
- Niendorf, T., Dijkhuizen, R.M., Norris, D.G., Campagne, M.V., Nicolay, K., 1996. Biexponential diffusion attenuation in various states of brain tissue: implications for diffusion-weighted imaging. *Magn. Reson. Med.* 36, 847–857.
- Özarslan, E., Shepherd, T.M., Vemuri, B.C., Blackband, S.J., Mareci, T.H., 2006. Resolution of complex tissue microarchitecture using the diffusion orientation transform (DOT). *NeuroImage* 31, 1086–1103.
- Pajevic, S., Basser, P.J., 2003. Parametric and non-parametric statistical analysis of DT-MRI data. *J. Magn. Reson.* 161, 1–14.
- Papadakis, N.G., Martin, K.M., Mustafa, M.H., Wilkinson, I.D., Griffiths, P.D., et al., 2002. Study of the effect of CSF suppression on white matter diffusion anisotropy mapping of healthy human brain. *Magn. Reson. Med.* 48, 394–398.
- Parker, G., Jones, D.K., 2011. Fibres at the Magic Angle Generated by Inappropriate 192 Calibration (MAGIC). *Proceedings of the International Society for Magnetic Resonance in Medicine*, Montreal, p. 1921.
- Parker, G., Jones, D.K., 2012. Pitfalls in the Reconstruction of Fibre ODFs Using Spherical Deconvolution of Diffusion MRI Data. *Proceedings of the International Society for Magnetic Resonance in Medicine*, Melbourne, p. 3588.
- Pasternak, O., Sochen, N., Gur, Y., Intrator, N., Assaf, Y., 2009. Free water elimination and mapping from diffusion MRI. *Magn. Reson. Med.* 62, 717–730.
- Patel, V., Shi, Y., Thompson, P.M., Toga, A.W., 2010. Mesh-based spherical deconvolution: a flexible approach to reconstruction of non-negative fiber orientation distributions. *NeuroImage* 51, 1071–1081.
- Pfefferbaum, A., Adalsteinsson, E., Sullivan, E., 2005. Frontal circuitry degradation marks healthy adult aging: evidence from diffusion tensor imaging. *NeuroImage* 26, 891–899.
- Pierpaoli, C., Jones, D.K., 2004. Removing CSF contamination in brain DT-MRIs by using a two-compartment tensor model. *Proceedings of the International Society for Magnetic Resonance in Medicine*, Kyoto, p. 1215.
- Pierpaoli, C., Jezzard, P., Basser, P.J., Barnett, A., DiChiro, G., 1996. Diffusion tensor MR imaging of the human brain. *Radiology* 201, 637–648.
- Pierpaoli, C., Marengo, S., Rohde, G., Jones, D.K., Barnett, A., 2003. Analyzing the contribution 1929 of cardiac pulsation to the variability of quantities derived from the diffusion tensor. *Proceedings of the International Society for Magnetic Resonance in Medicine*, Toronto, pp. 70.
- Pruessmann, K., Weiger, M., Scheidegger, M., Boesiger, P., 1999. SENSE: sensitivity encoding for fast MRI. *Magn. Reson. Med.* 42, 952–962.
- Pugliese, L., Catani, M., Ameis, S., Dell'Acqua, F., de Schotten, M.T., et al., 2009. The anatomy of extended limbic pathways in Asperger syndrome: a preliminary diffusion tensor imaging tractography study. *NeuroImage* 47, 427–434.
- Qiu, A., Zhong, J., Graham, S., Chia, M.Y., Sim, K., 2009. Combined analyses of thalamic volume, shape and white matter integrity in first-episode schizophrenia. *NeuroImage* 47, 1163–1171.
- Qiu, A., Tuan, T.A., Woon, P.S., Abdul-Rahman, M.F., Graham, S., et al., 2010. Hippocampal-cortical structural connectivity disruptions in schizophrenia: an integrated perspective from hippocampal shape, cortical thickness, and integrity of white matter bundles. *NeuroImage* 52, 1181–1189.
- Raffelt, D., Tournier, J.D., Rose, S., Ridgway, G.R., Henderson, R., et al., 2012. Apparent fibre density: a novel measure for the analysis of diffusion-weighted magnetic resonance images. *NeuroImage* 59, 3976–3994.
- Ronen, I., Kim, K.H., Garwood, M., Ugurbil, K., Kim, D.S., 2003. Conventional DTI vs. slow and fast diffusion tensors in cat visual cortex. *Magn. Reson. Med.* 49, 785–790.
- Roosendaal, S.D., Geurts, J.J.G., Vrenken, H., Hulst, H.E., Cover, K.S., et al., 2009. Regional DTI differences in multiple sclerosis patients. *NeuroImage* 44, 1397–1403.
- Rosas, H.D., Lee, S.Y., Bender, A.C., Zaleta, A.K., Vangel, M., et al., 2010. Altered white matter microstructure in the corpus callosum in Huntington's disease: implications for cortical "disconnection". *NeuroImage* 49, 2995–3004.
- Sakaie, K.E., Lowe, M.J., 2007. An objective method for regularization of fiber orientation distributions derived from diffusion-weighted MRI. *NeuroImage* 34, 169–176.
- Setsompop, K., Gagoski, B.A., Polimeni, J., Witzel, T.W., V.J., Wald, L.L., 2012. Blipped-Controlled Aliasing in Parallel Imaging (blipped-CAIPI) for simultaneous multi-slice EPI with reduced g-factor penalty. *Magn Reson Med* 67, 1210–1224.
- Sled, J., Pike, G., 2001. Quantitative imaging of magnetization transfer exchange and relaxation properties *in vivo* using MRI. *Magn. Reson. Med.* 46, 923–931.
- Song, S.K., Sun, S.W., Ramsbottom, M.J., Chang, C., Russell, J., et al., 2002. Demyelination revealed through MRI as increased radial (but unchanged axial) diffusion of water. *NeuroImage* 17, 1429–1436.
- Stepisnik, J., 1981. Analysis of NMR self-diffusion measurements by a density matrix calculation. *Physica B & C* 104, 350–364.
- Stricker, N.H., Schweinsburg, B.C., Delano-Wood, L., Wierenga, C.E., Bangen, K.J., et al., 2009. Decreased white matter integrity in late-myelinating fiber pathways in Alzheimer's disease supports retrogenesis. *NeuroImage* 45, 10–16.
- Sullivan, E., Pfefferbaum, A., 2006. Diffusion tensor imaging and aging. *Neurosci. Biobehav. Rev.* 30, 749–761.
- Takahashi, M., Hackney, D.B., Zhang, G.X., Wehrli, S.L., Wright, A.C., et al., 2002. Magnetic resonance microimaging of intraaxonal water diffusion in live excised lamprey spinal cord. *Proc. Natl. Acad. Sci. U. S. A.* 99, 16192–16196.
- Takeuchi, H., Taki, Y., Sassa, Y., Hashizume, H., Sekiguchi, A., et al., 2010. White matter structures associated with creativity: evidence from diffusion tensor imaging. *NeuroImage* 51, 11–18.
- Tournier, J.D., Calamante, F., Gadian, D., Connelly, A., 2004. Direct estimation of the fiber orientation density function from diffusion-weighted MRI data using spherical deconvolution. *NeuroImage* 23, 1176–1185.
- Tournier, J.D., Calamante, F., Connelly, A., 2007. Robust determination of the fibre orientation distribution in diffusion MRI: non-negativity constrained super-resolved spherical deconvolution. *NeuroImage* 35, 1459–1472.
- Tournier, J.D., Calamante, F., Connelly, A., 2009. How many diffusion gradient directions are required for HARDI? *Proc. Int. Soc. Magn. Reson. Med.* 17, 358.
- Tournier, J.D., Mori, S., Leemans, A., 2011. Diffusion tensor imaging and beyond. *Magn. Reson. Med.* 65, 1532–1556.
- Tristán-Vega, A., Westin, C-F., Aja-Fernández, S., 2009. Estimation of fiber orientation density probability density functions in high angular resolution diffusion imaging. *NeuroImage* 47, 638–650.
- Tristán-Vega, A., Aja-Fernández, S., Westin, C-F., 2012. Least squares for diffusion tensor estimation revisited: propagation of uncertainty with Rician and non-Rician signals. *NeuroImage* 59 (4), 4032–4043.
- Tuch, D.S., 2004. Q-ball imaging. *Magn. Reson. Med.* 52, 1358–1372.
- Tuch, D.S., Reese, T., Wiegell, M., Makris, N., Belliveau, J., et al., 2002. High angular resolution diffusion imaging reveals intravoxel white matter fiber heterogeneity. *Magn. Reson. Med.* 48, 577–582.
- van Kampen, N., 1974. Cumulant expansion for stochastic linear-differential equations I. *Physica* 74, 215–238.
- Vos, S.B., Jones, D.K., Viergever, M.A., Leemans, A., 2011. Partial volume effect as a hidden covariate in DTI analyses. *NeuroImage* 55, 1566–1576.
- Wedeen, V.J., Hagmann, P., Tseng, W.Y.I., Reese, T.G., Weisskoff, R.M., 2005. Mapping complex tissue architecture with diffusion spectrum magnetic resonance imaging. *Magn. Reson. Med.* 54, 1377–1386.
- Wheeler-Kingshott, C.A.M., Cercignani, M., 2009. About "axial" and "radial" diffusivities. *Magn. Reson. Med.* 61, 1255–1260.
- Whitcher, B., Tuch, D.S., Wisco, J.J., Sorensen, A.G., Wang, L.Q., 2008. Using the wild bootstrap to quantify uncertainty in diffusion tensor imaging. *Hum. Brain Mapp.* 29, 346–362.
- White, N.S., Dale, A.M., 2009. Optimal diffusion MRI acquisition for fiber orientation density estimation: an analytic approach. *Hum. Brain Mapp.* 30, 3696–3703.
- Wiest-Daessle, N., Prima, S., Coupe, P., Morrissey, S.P., Barillot, C., 2008. Rician noise removal by non-local means filtering for low signal-to-noise ratio MRI: applications to DT-MRI. In: Metaxas, D., Axel, L., Szekely, G., Fichtinger, G. (Eds.), *Medical Image Computing and Computer-Assisted Intervention – Miccai 2008*, Pt II, Proceedings, pp. 171–179.
- Wimberger, D.M., Roberts, T.P., Barkovich, A.J., Prayer, L.M., Moseley, M.E., et al., 1995. Identification of premyelination by diffusion-weighted MRI. *J. Comput. Assist. Tomogr.* 19, 28–33.